AN ASSESSMENT OF REGIONAL CLIMATE TRENDS AND CHANGES TO THE MT. JAYA GLACIERS OF IRIAN JAYA

A Thesis

by

JONI L. KINCAID

Submitted to the Office of Graduate Studies of
Texas A&M University
in partial fulfillment of the requirements for the degree of

MASTER OF SCIENCE

May 2007

Major Subject: Geography

AN ASSESSMENT OF REGIONAL CLIMATE TRENDS AND CHANGES TO THE MT. JAYA GLACIERS OF IRIAN JAYA

A Thesis

by

JONI L. KINCAID

Submitted to the Office of Graduate Studies of
Texas A&M University
in partial fulfillment of the requirements for the degree of

MASTER OF SCIENCE

Approved by:

Chair of Committee,	Andrew G. Klein
Committee Members,	John R. Giardino
	Hongxing Liu
Head of Department,	Douglas J. Sherman

May 2007

Major Subject: Geography

ABSTRACT

An Assessment of Regional Climate Trends and Changes

to the Mt. Jaya Glaciers of Irian Jaya. (May 2007)

Joni L. Kincaid, B.A., The University of Texas

Chair of Advisory Committee: Dr. Andrew G. Klein

Over the past century, glaciers throughout the tropics have predominately retreated. These small glaciers, which respond quickly to climate changes, are becoming increasingly important in understanding glacier-climate interactions. The glaciers on Mt. Jaya in Irian Jaya, Indonesia are the last remaining tropical glaciers in the Western Pacific region. Although considerable research exists investigating the climatic factors most affecting tropical glacier mass balance, extensive research on the Mt. Jaya glaciers has been lacking since the early 1970s.

Using IKONOS satellite images, the ice extents of the Mt. Jaya glaciers in 2000, 2002, 2003, 2004, and 2005 were mapped. The mapping indicates that the recessional trend which began in the mid-19th century has continued. Between 1972 (Allison, 1974; Allison and Peterson, 1976) and 2000, the glaciers lost approximately 67.6% of their area, representing a reduction in surface ice area from 7.2 km^2 to 2.35 km^2. From 2000 to 2005, the glaciers lost an additional 0.54 km^2, representing approximately 24% of the 2000 area. Rates of ice loss, calculated from area measurements for the Mt. Jaya glaciers in 1942, 1972, 1987, and 2005, indicate that ice loss on Mt. Jaya has increased during each subsequent period.

Preliminary modeling, using 600 hPa atmospheric temperature, specific humidity, wind speeds, surface precipitation, and radiation values, acquired from the NCEP Reanalysis dataset, indicates that the only climate variable having a statistically-significant change with a magnitude great enough to strongly affect ice loss on these glaciers was an increase in the mean monthly atmospheric temperature of 0.24°C between 1972 and 1987. However, accelerated ice loss occurring from 1988-2005 without large observed changes in the weather variables indicates that a more complex explanation may be required. Small, though statistically-significant changes were found in regional precipitation, with precipitation decreasing from 1972-1987 and increasing from 1988-2005. While, individually, these changes were not of sufficient magnitude to have greatly affected ice loss on these glaciers, increased precipitation along with a rising freezing level may have resulted in a greater proportion of the glacier surface being affected by rain. This may account for the increased recession rate observed in the latter period.

I dedicate this thesis to my children, Tiffany Guild, Amber Dunckel, and Clinton Dunckel, and to my mother, Sherry Ann Kincaid, for their patience, understanding, and encouragement during this process. I also dedicate this thesis to the memory of my father, Joseph David Kincaid, who always believed in me. I would not be who I am today if not for my family. I am extremely grateful.

ACKNOWLEDGMENTS

Becoming a scientist has been a dream of mine since I was a young girl and, therefore, the act of researching, writing, and especially, completing my thesis has been a particularly rewarding experience for me. I do not believe I could have brought this dream to fruition without the assistance and support from many people. First, I would like to thank the staff in the Department of Geography for their hard work in taking care of all of the little details and their smiling faces no matter what request I made of them. I would also like to thank Dr. Doug Sherman, our Department Head, Dr. Jonathon Smith, our Assistant Department Head, and Dr. Dave Cairns, our Graduate Advisor for their support and advice. All of the professors in this department have assisted me, but I especially want to acknowledge Dr. Sarah Bednarz and Dr. Robert Bednarz for their encouragement and counsel.

I would like to thank my committee chair, Dr. Andrew Klein, who went beyond the call of duty in advising me. He provided me the tools required to complete my thesis, made sure that I always had funding resources, and supported me in my professional development. Because of him I have already met many significant scientists in my field and contributed to outside projects. He encouraged me to think independently and to make my projects my own. His example and the opportunities he afforded me have greatly enhanced my perception of myself as a scientist.

I want to acknowledge my other committee members, Dr. Rick Giardino and Dr. Hongxing Liu. Although Dr. Giardino is very busy as the Dean of Graduate Studies and

also has his own students to advise, he always took time to meet with me, advise me, and spent a lot of time trying to teach me how to write. He also provided me with invaluable field experience, where I not only learned many new things, but also gained confidence in my ability to perform fieldwork and work as a team. I want to thank him for going beyond what was required for a committee member and strengthening my development as a researcher.

I want to thank Dr. Liu for always making me feel welcome within the remote sensing team here in the Department of Geography and encouraging us graduate students to help each other in achieving success. His example of selflessness, work ethic and his high professional standards has served to motivate me on many occasions. I always found his door open whenever I needed assistance, many times even at one o'clock in the morning.

I have been provided with many sources of funding that enabled me to complete this thesis, and I would like to thank all of them. I thank the Department of Geography for my teaching assistantship, Dr. Eric Lindquist at The Institute for Science, Technology, and Public Policy at the George Bush School of Government and Public Service and Dr. Andrew Klein in the Department of Geography for my research assistantships, and Dr. Sarah Bednarz in the Department of Geography for my National Science Foundation Fellowship. Each of these positions were invaluable to my professional development, not only because of the knowledge I gained from them, but also because of the respect, support, and professional mentoring that each of these scientists provided me.

I would like to acknowledge all of the geography graduate students who have stopped their own work to assist me with a research problem or to edit my manuscripts over the past few years. I would especially like to thank Gabriel Burns, Zheng Cheng, Matthew Clemonds, Adriana Martinez, Lei Wang, Tavia Prouhet, Michelle Simms, Sheng-Jung Tang, and Nikki Williams for their help.

I would have gone crazy attempting to complete this task without the moral support I received from many of my friends, but especially Serena Aldrich, Jose Gavinha, Courtney Harmon, Tracey Hayes, and Sandra Metoyer. Their support was invaluable.

TABLE OF CONTENTS

Page

ABSTRACT iii

DEDICATION v

ACKNOWLEDGMENTS vi

TABLE OF CONTENTS ix

LIST OF FIGURES xii

LIST OF TABLES xiv

1. INTRODUCTION 1

    1.1. Thesis Objectives 3

2. THE STUDY SITE: MT. JAYA IN IRIAN JAYA, INDONESIA 5

    2.1. Descriptions of the Mt. Jaya Glaciers 5
        2.1.1 The Valley Glaciers 5
        2.1.2 The Northwall Firn 8
    2.2. History of Field Excursions to the Area 9

3. BACKGROUND 10

    3.1. Glacier Regimes of the Tropics 10
    3.2. Inner Tropical Glaciers and Climate Change 11
    3.3. El Niño Southern Oscillation (ENSO) Effects on Tropical Glaciers 12

4. DATA SOURCES 14

    4.1. IKONOS Images 14
    4.2. Advanced Spaceborne Thermal Emission and Reflection Radiometer (ASTER) Images 16
    4.3. Landsat TM and ETM+ Images 16
    4.4. Topography of the Mt. Jaya Glacier Area 17

Page

4.5. National Centers for Environmental Prediction/National Center for Atmospheric Research (NCEP/NCAR) Reanalysis Data 19
4.6. Oceanic Niño Index (ONI) 20
4.7. Historical Data 20
4.7.1. Glacier Extents from ca. 1850-1972 21
4.7.2. Glacier Extents from 1972-1987 23

5. METHODS 25

5.1. Acquisition of Satellite Images 25
5.2. Preprocessing Satellite Images: Band Selection for Color Composites 32
5.3. Coregistration of the Satellite Images 35
5.3.1. IKONOS Images 35
5.3.2. ASTER Image 36
5.3.3. Landsat TM and ETM+ Images 36
5.4. Glacial Boundary Mapping 37
5.4.1. Mapping from the IKONOS Images 38
5.4.2. Mapping from the ASTER Image 41
5.4.3. Mapping from the Landsat TM and ETM+ Images 41
5.5. Comparing Historical Extents with 2000 to 2005 Surface Areas 42
5.6. Climate Data Analysis 43

6. RESULTS 45

6.1. 2000 to 2005 Mapping Results 45
6.2. Results from Comparing the 1972 and 1987 Glacier Areas to the 2000 to 2005 Areas 52
6.3. Climate Analysis Results 53
6.3.1. Frequency and Magnitude of El Niño 53
6.3.2. Analysis of the Meteorological Variables 56
6.3.3. Climate Variables and ENSO 58

7. DISCUSSION 61

7.1. Comparisons of the Mapping Results Obtained Using ASTER and Landsat ETM+ Images 61
7.2. Overall Changes in Glacier Extents on Mt. Jaya from ca. 1850 to 2005 61
7.2.1. Description of Tables and Figures Compiling Observations from ca. 1850-2005 61

Page

7.3. Detailed Changes for the Northwall Firn and Meren Glacier System 67
7.3.1. E. Northwall Firn/Meren Glacier System 69
7.3.2. W. Northwall Firn 71
7.4. Detailed Changes for the Carstensz Glacier System 72
7.5. The Rates of Recession for the Mt. Jaya Glaciers are Accelerating 73
7.6. Relationship of Climate Variables to Glacial Recession 76

8. CONCLUSIONS 78

REFERENCES 83

VITA 87

LIST OF FIGURES

FIGURE		Page
1	Site map for the Mt. Jaya glaciers	6
2	The Mt. Jaya glaciers in 1972	7
3	Topography of the Mt. Jaya area	18
4	Original 2000 IKONOS image of the Mt. Jaya glaciers	26
5	Original 2002 IKONOS image of the Mt. Jaya glaciers	27
6	Original 2003 ASTER image of the Mt. Jaya glaciers	28
7	Original 2003 Landsat ETM+ image of the Mt. Jaya glaciers	29
8	Original 2004 Landsat TM image of the Mt. Jaya glaciers	30
9	Original 2005 Landsat TM image of the Mt. Jaya glaciers	31
10	Subsets of the IKONOS images after processing	33
11	Subsets of the coregistered ASTER and Landsat composites	34
12	Distinguishing ice from rock	39
13	Mapping the Carstensz tail	40
14	Ice loss for the Mt. Jaya glaciers from 2000 to 2002	46
15	Ice loss for the Mt. Jaya glaciers from 2000 to 2003	47
16	Ice loss for the Mt. Jaya glaciers from 2003 to 2005	48
17	Ice loss for the Mt. Jaya glaciers from 2000 to 2005	49
18	Glacier recession on Mt. Jaya, Indonesia in 1972, 1987, 2000, and 2005	54
19	Oceanic Niño Index and ENSO events	55

FIGURE Page

20 Mean monthly Oceanic Niño Index anomalies during each period for La Niña, neutral, and El Niño months, respectively, from 1951 to 2005 57

21 Monthly means for temperature, freezing level, precipitation, incoming radiation, wind magnitude, specific humidity, and percent cloud cover during each time period 59

22 Surface ice areas for the Mt. Jaya glaciers from ca. 1850 to 2005 68

23 Hypsometries for the W. Northwall Firn, the E. Northwall Firn/Meren glacier system, and the Carstensz glacier for 1972, 1987, and 2002 70

24 Surface ice areas for the Northwall Firn and Meren glacier from 1936 to 2005 75

LIST OF TABLES

TABLE		Page
1	Spectral and spatial characteristics of the IKONOS, ASTER, and Landsat TM and ETM+ images	15
2	Surface ice areas for the Mt. Jaya glaciers from 2000 to 2005	50
3	Climate changes from 1951-2005	60
4	Ice surface areas for the Mt. Jaya glaciers from ca. 1850 to 2005	62
5	Ice surface areas for individual glaciers comprising the Northwall Firn/Meren glacier system from ca. 1850 to 2005	63
6	Ice surface areas for the individual glaciers comprising the Carstensz glacier system from ca. 1850 to 2005	64
7	Rates of ice loss for the Mt. Jaya glaciers from ca. 1850 to 2005	66

1. INTRODUCTION

Tropical glaciers are important indicators of climate change and provide valuable information on past climate conditions. However, there are fundamental gaps in the current body of research on glaciers that thwart a more complete understanding of glacial processes in relation to global climate change. First, long-term records of glacial change need to be established for glaciers (Houghton and others, 2001). Mass balance and climate observations are scarce or completely lacking for most glaciers, and observations that have been made commonly cover only short time periods (Braithewaite and Zhang, 1999; Dyurgerov and Meier, 2000). This is partially a result of inaccessibility, as glacial environments are generally remote, and harsh climate conditions offer few opportunities for investigation.

Second, more individual case studies are required because glaciers located in diverse geographical regions respond differently to various climatic factors (Braithewaite and Zhang, 1999; Francou and others, 2003). Overall, the synchronicity of mass balance changes in temperate and tropical glaciers indicates that rising atmospheric temperatures are the global cause for glacier recession (Kaser, 2001). However, the relationships between glaciers and tropical climate are complex and simple explanations for change should not be overstated. Therefore, additional studies must be completed to provide more detailed causal explanations (Kaser, 2001). Indicative of this oversimplification, it was reported in the contribution of Working Group I to the Third Assessment Report of

---

This thesis follows the style of *Journal of Glaciology*.

the Intergovernmental Panel on Climate Change (IPCC) (Houghton and others, 2001) that tropical glaciers have experienced accelerated rates of recession over the past century that are inconsistent with the warming trend in the region for the same period. Whereas, Kaser and Osmaston (2002) note several excellent studies on tropical glaciers, they state that these glacier studies are based on those that have been completed in the Alps and, thereby, remain "alpine-centric" for lack of sufficient research on tropical glaciers.

To counter these gaps in the knowledge base and to improve overall understanding of climate-glacier interactions the IPCC report indicated a directive for future research. First, priority should be given to acquiring data on glaciers that have established long-term records. Second, remote sensing techniques should be established for long-term glacial monitoring. Third, research should focus on a few glaciers from different climatic regions to maximize efforts. And fourth, energy balance and glacier geometry models should be improved so that knowledge of climate-glacier interactions can advance more rapidly.

Following the delimitation of tropical glacier regions set forth by Kaser (2001), tropical glaciers currently exist in South America, East Africa, and in Indonesia. Recent studies of tropical glaciers have primarily focused on a few glaciers located in the Andes (Francou and others, 1995; Kaser, 2001; Ramírez and others, 2001; Francou and others, 2003; Favier and others, 2004a; Francou and others, 2004; Georges, 2004) in South America; and on Mt. Kenya (Mölg and others, 2003; Mölg and Hardy, 2004) in Africa. However, extensive studies of the Mt. Jaya glaciers in Indonesia have not been

completed since 1972. These glaciers differ from other tropical glaciers not only in geographic location, but also in that a historical record of changes exists for these glaciers extending from 1913 to 1987. Following the directives from the last IPCC report, this thesis extends the record for glacial change on Mt. Jaya using satellite images and tests whether or not the recession of these tropical glaciers is in fact accelerating. Secondarily, regional climate trends, as well as the Oceanic Niño Index (ONI) will be examined and statistical techniques are used to provide an overview of the general climate conditions existing in the region from 1951 to 2005.

The glacial mapping done as part of this thesis will be provided to the World Glacier Monitoring Service (WGMS) and the Global Land Ice Measurements from Space (GLIMS), a collaborative project involving over sixty institutions including the National Aeronautics and Space Administration (NASA), United States Geological Survey (USGS), and the National Snow and Ice Data Center.

1.1. Thesis Objectives

The objectives of this thesis are to: (1) map and measure the area extents for the Mt. Jaya glaciers for May 2000, June 2002, May 2003, July 2004, and June 2005, (2) evaluate the changes in surface ice area for the Mt. Jaya glaciers from ca. 1850 to June 2005 by combining our time series with historical observations, and (3) compare and contrast the meteorological record for Irian Jaya and ONI with the surface ice area changes for the Mt. Jaya glaciers using National Centers for Environmental Prediction/National Center for Atmospheric Research reanalysis data.

The purpose for objective one is to extend the historical database of surface ice measurements for these important glaciers and objective two tests whether or not the Mt. Jaya glaciers have receded at an accelerating rate over the past century as indicated by the last IPCC report. Several valuable studies on climate-glacier interactions have been completed on tropical glaciers in South America and Africa since 1972, when the last detailed studies for the Mt. Jaya glaciers occurred. Therefore, the last objective of this thesis will test whether or not the findings from these studies are transferable to the Mt. Jaya glaciers which are located in a climatically different location.

2. THE STUDY SITE: MT. JAYA IN IRIAN JAYA, INDONESIA

The Mt. Jaya glaciers are located in Irian Jaya, Indonesia at latitude 4°05'S and longitude 137°11'E. The peaks of Mt. Jaya reach 4884 m and are part of a west-northwest and east-southeast trending mountain range that extends across the island of New Guinea (Allison, 1974) (Fig. 1).

2.1. Descriptions of the Mt. Jaya Glaciers

In 1972, five ice masses existed on Mt. Jaya: the Carstensz glacier system, which included the Wollaston and Van de Water glaciers, the Meren glacier, the Southwall Hanging glacier, and the east and west sections of the Northwall Firn glacier (Allison, 1974; Allison and Peterson, 1976). The following two sections summarize the descriptions of the glaciers provided by Allison (1974) and Allison and Peterson (1976) based on their field observations in 1972 (Fig. 2).

2.1.1. The Valley Glaciers

The Meren and Carstensz glaciers are valley glaciers flowing westward into the Meren and Yellow Valleys, respectively. These valley glaciers lie on the southern side of the range and are separated only by a very narrow ridge. In 1972, the Carstensz flowed from a peak (the Carstensz Top) with a vertical extent ranging from 4800 m down to 4380 m. The Meren glacier flowed from a peak at 4862 m located within the E. Northwall Firn, as well as from an area at the head of the valley that Dozy (1938) referred to as the Middle Firn, to a minimum elevation of about 4260 m. There are not many details

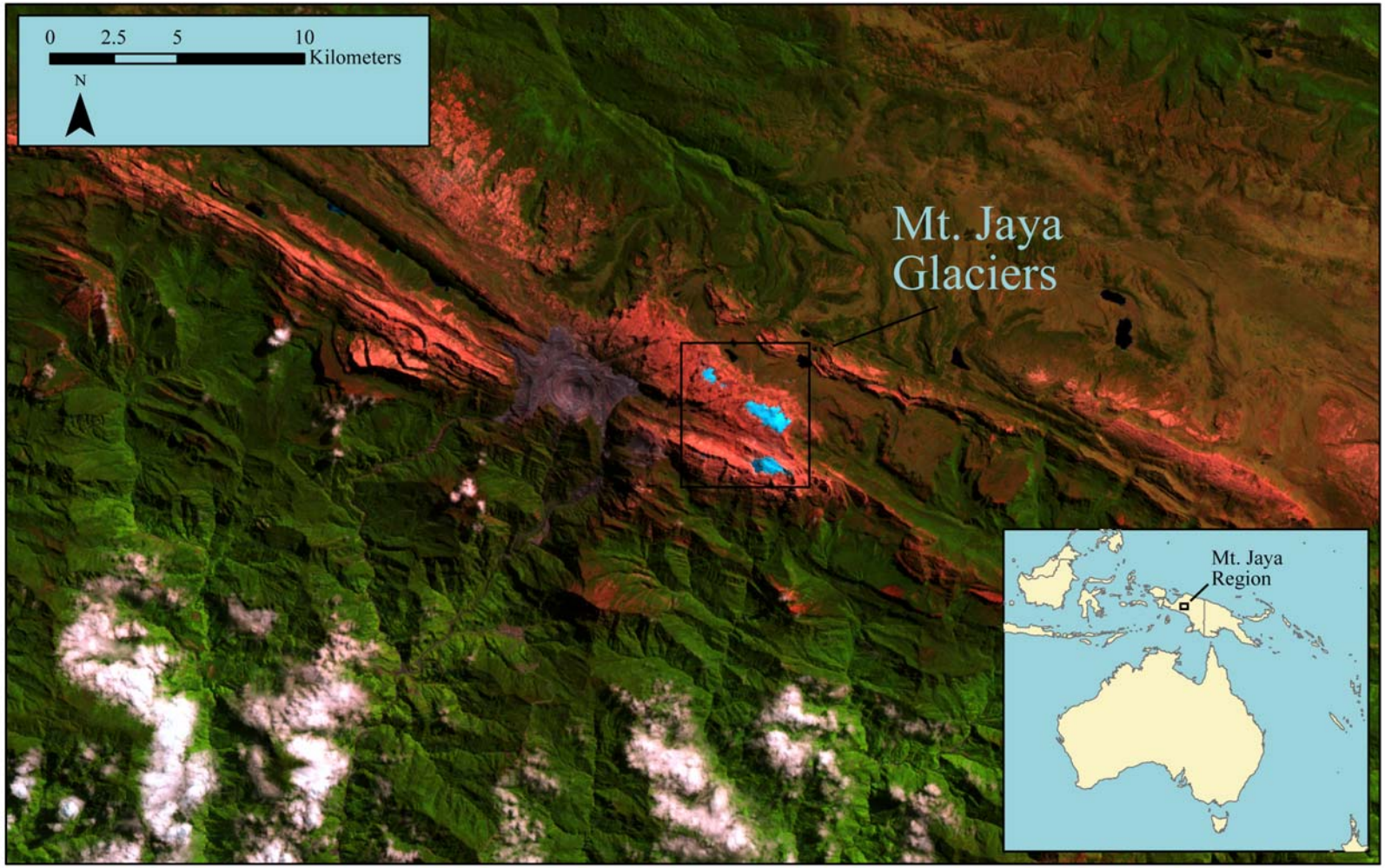

Fig. 1. Site map for the Mt. Jaya glaciers. The Mt. Jaya glaciers are located in Irian Jaya, Indonesia on the western half of the island of New Guinea. The large circular feature to the left of the glaciers is a gold and copper mine. This map was created using a Landsat TM scene taken on July 26, 2004.

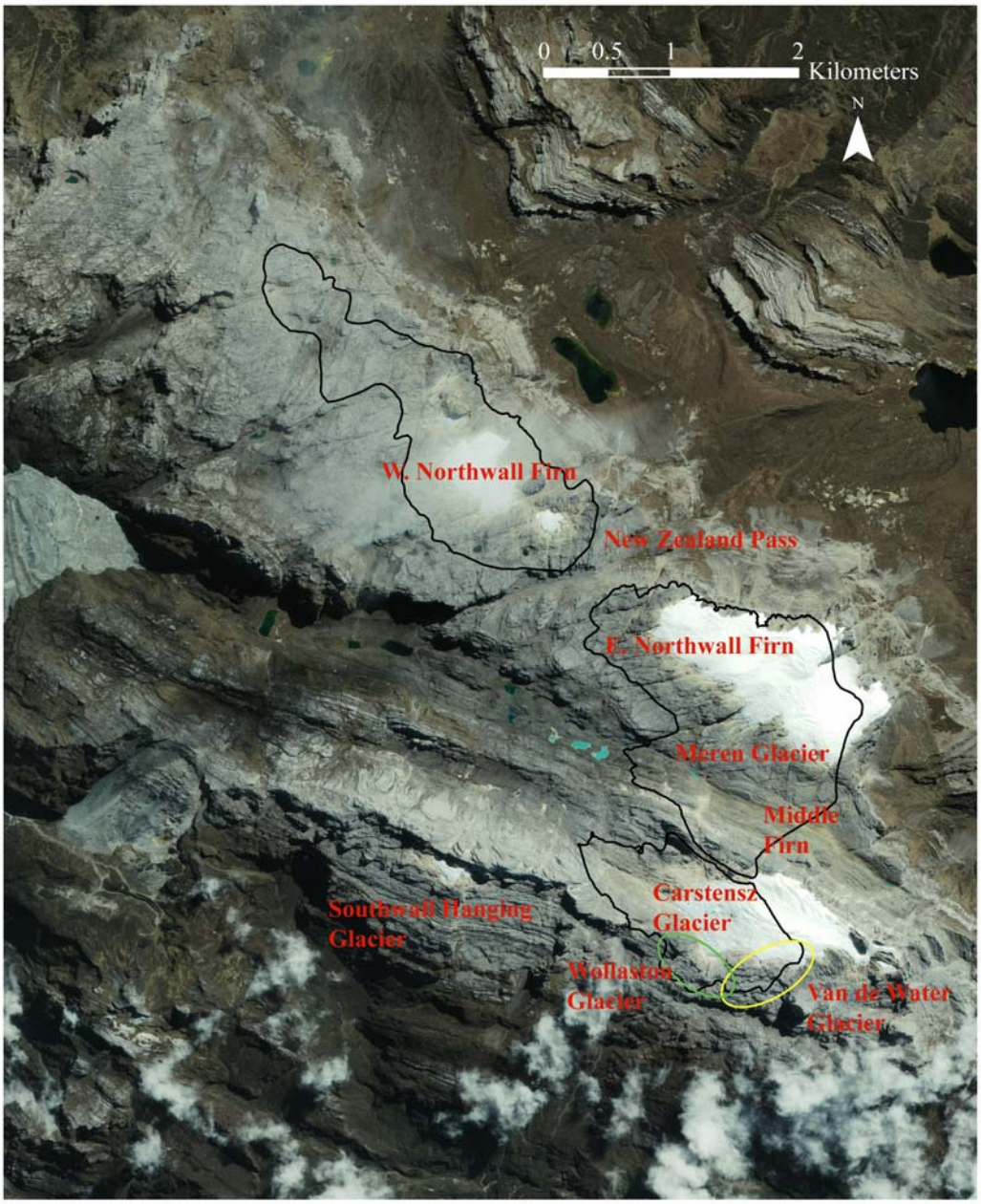

Fig. 2. The Mt. Jaya glaciers in 1972. The black outlines indicate the extent of the glaciers as mapped during the Australian Universities' field expeditions in 1972 (Hope and others, 1976). The yellow and green circles denote the general areas of the Carstensz glacier designated as the Van de Water and Wollaston glaciers. The base image is an IKONOS image acquired by the sensor on June 11, 2002.

provided for the smaller Harrer, Wollaston, and Van de Water glaciers, which from all reports, were quite small in area even at the beginning of the 20th century. However, the Harrer glacier extended east from the Middle Firn, the Van de Water glacier extended down the southern wall of the head of the Carstensz glacier, and the Wollaston glacier flowed off of the Carstensz from its southern border. These small glaciers were limited in size by the precipitous cliffs over which the glaciers flowed.

The Southwall Hanging glaciers were small glaciers that flowed over a cliff along the southern ridge of the Yellow Valley just west of the Carstensz glacier. Approximately a hundred glaciers comprised the Southwall Hanging glaciers giving the cliff an apron-like appearance. Similar to the Harrer, Wollaston, and Van de Water glaciers, these glaciers were limited in size due to the steep topography of the south face of the mountain.

2.1.2. The Northwall Firn

The E. Northwall Firn lies along a ridge, north of the Meren Valley, extending from a mountain peak to the east to the New Zealand Pass on the west and covers an elevation range of 4520-4810 m. The W. Northwall Firn is a long, very narrow firn field (approximately 3.5 km in length and averaging 0.7 km in width) extending west from the New Zealand Pass along the same ridge as the E. Northwall Firn. The W. Northwall Firn covers an elevation range of 4510-4750 m.

2.2. History of Field Excursions to the Area

The Mt. Jaya glaciers were first observed in 1623 by Jan Carstensz (Allison, 1974). Since then visits on record to the glaciers were made by Wollaston in 1913 (Wollaston, 1914), Colijn and Dozy in 1936 (Dozy, 1938), and by a climbing team in 1962 (Harrer, 1965). Each of these field excursions resulted in the acquisition of surface area measurements for at least one or more of the glaciers.

The Australian Universities' expeditions to the glaciers in the early 1970s involved extensive field research, resulting in not only mass balance measurements for 1972-1973 for the Carstensz and Meren glaciers, but also, measurements of surface areas for all of the ice fields (Allison, 1974; Allison and Peterson, 1976). Climate data (Allison and Bennett, 1976), a topographic survey derived trigometrically (Peterson and others, 1973), and detailed descriptions of other aspects of the area, such as geomorphic and botanical features (Hope and others, 1976) were also made and served to support further research on the glaciers. After the 1972-1973 field excursions, several other measurements of the surface areas of the Mt. Jaya glaciers were made primarily using satellite images (Allison and Peterson, 1989; Peterson and Peterson, 1994; Klein and Kincaid, 2006). The 2000-2002 measurements obtained from this thesis have already been published (Klein and Kincaid, 2006). In addition, this thesis further extends the record for the 2003-2005 periods.

3. BACKGROUND

3.1. Glacier Regimes of the Tropics

Three distinct glacier regimes: subtropical, inner and outer, exist within the tropics (Kaser, 1999). According to Kaser (1999), subtropical glaciers, located in the southwestern portion of Bolivia and in northern Chile, exist in arid environments. Changes in the mass balance of subtropical glaciers are greatly affected by high sublimation rates (Favier and others, 2004b). At the other extreme, the inner tropical environment is wet and humid with negligible seasonal variation in precipitation and temperature (Kaser, 2001). These inner tropical glaciers are found in the Ruwenzori Range, located in Uganda (Kaser, 2001), in the lower latitudes of the Andes, such as in Ecuador (Favier and others, 2004b), and in Irian Jaya, Indonesia (Kaser, 2001). Intermediate to these two glacier regions is the outer tropics, where climate-glacier relationships most resemble those of temperate glaciers. Outer tropical glaciers are characterized by distinct wet and dry seasons and are located in the Cordillera Blanca, Peru (Kaser, 2001) and the Cordillera Real, Bolivia, and include the Zongo (Favier and others, 2004b), Chacaltaya (Ramírez and others, 2001), and the Illimani (Wagnon and others, 2003) glaciers. The majority of tropical glaciers are located in the outer tropics, and to date, research has predominantly focused on outer tropical glacier-climate interactions.

3.2. Inner Tropical Glaciers and Climate Change

Kaser (1999) suggests that, whereas atmospheric vapor and temperature have been indicated as the climate factors primarily controlling tropical glacier change, a complex interplay of climate variables best explains the observed glacier recession. However, only a few recent studies (Kaser, 2001; Mölg and others, 2003; Francou and others, 2004; Favier and others, 2004a, 2004b), specific to the inner tropics, have focused on glacier-climate relationships that are relevant to Irian Jaya. Overall, theoretically modeling of the vertical mass balance profile of inner tropical glaciers suggest that these glaciers are highly sensitive to changes in air temperature (Klein and others, 1999; Kaser, 2001).

Studies on the Antizana 15 glacier in Ecuador indicate that air temperature controls the precipitation phase (snow versus rain), and therefore, is the primary control on mass balance (Favier and others, 2004a, 2004b; Francou and others, 2004). Overall, one-quarter of the precipitation occurs as rain over the glacier, decreasing albedo, and subsequently increasing melt (Favier and others, 2004a).

Hastenrath and Kruss (1992) suggest that, on the equatorial African glaciers of Mt. Kenya, incoming solar radiation was the major control for glacier recession occurring between 1899 and 1963. However, this could not account for ice thinning which occurred uniformly over the glaciers between 1963 and 1987. Sensitivity analyses indicated that increases in specific humidity resulting in increased energy available for melt was the cause for the thinning ice. A radiation modeling study, by Mölg and others

(2003), on the glaciers in the Rwenzori range suggests that increases in short-wave radiation are the primary cause of recession for these glaciers.

For the Mt. Jaya glaciers, Allison and Kruss (1977) successfully constructed a flow-line model of the Carstensz glacier to determine possible causes for the observed retreat in the area. The results from this model indicated that a temperature change of 0.6°C over the past century, which corresponded well with overall estimated tropical climate changes from 1870 to 1940, best reflected the glacier recession that had occurred over the same time period. However, according to Allison and Kruss (1977), their model primarily investigated temperature and precipitation, and therefore, they did not rule out other climate factors that could be affecting the glaciers. Some lines of evidence indicated that net radiation was of primary importance in the higher melt rates for the Meren glacier. In 1972, the tongue of the Meren glacier was covered quite heavily by cryo-algae and numerous melt ponds, both of which resulted in lower albedos (Allison, 1974). Increased cloud cover, observed shortly before noon on most days, protected the western side of the Carstensz glacier from incoming solar radiation resulting in different elevations for the east and west sides of the snowline (Allison and Peterson, 1976).

3.3. El Niño Southern Oscillation (ENSO) Effects on Tropical Glaciers

The El Niño Southern Oscillation (ENSO) phase correlates well with the annual mass balance of Andean glaciers (Francou and others, 1995; Ramírez and others, 2001; Francou and others, 2004; Favier and others, 2004b; Georges, 2004). On these glaciers, El Niño years correspond with drier conditions, higher temperatures, and lower wind speeds (Francou and others, 2004). On the Antizana 15 glacier, the greatest impacts on

mass balance occurred between February and May during El Niño years indicating a three month lag time between sea surface anomalies controlling ENSO phase and corresponding climate changes in the Andes (Francou and others, 2004). In addition to drier conditions, a higher proportion of the reduced precipitation occurs as rain. Lower wind speeds also act to reduce sublimation rates on inner tropical glaciers by reducing the turbulent heat fluxes (Francou and others, 2003; Francou and others, 2004).

The opposite conditions occur during La Niña years and these conditions have been shown to induce small positive anomalies in the mass balance of Antizana 15 glacier (Francou and others, 2004). Although these studies have found correlations between ENSO phase and inner tropical glacier mass balance, Garreaud and others (2003) suggest that additional studies are required to understand thoroughly the connections. In their study of climate of the Altiplano, they found that some discrepancies existed in correlations between drier, warmer conditions and El Niño years. To this date, no studies have investigated the effect of ENSO on the Mt. Jaya glaciers.

4. DATA SOURCES

4.1. IKONOS Images

In 1999, the IKONOS sensor was launched and began collecting data from space (GeoEye, 2006). The IKONOS sensor is in a sun-synchronous orbit and acquires all images at approximately 10:30am local time. Facilitating change detection studies, this sensor collects data over the same geographical space once approximately every 3 days at 40° latitude, more frequently at higher latitudes, and less frequently near the equator (Grodecki and Dial, 2001). IKONOS acquires images at very high spatial resolutions of 1 m and 4 m for the panchromatic and multispectral bands, respectively (GeoEye, 2006). Overall, five spectral bands of data are collected covering the 0.45 to 0.90 micrometers spectral range (Table 1), and includes one panchromatic band, three visible infrared (VIR) bands, and one near infrared (NIR) band. The radiometric resolution is 8 bits for the multispectral bands and 11 bits for the panchromatic band. The high geometric and radiometric accuracy of these images, as well as the high spectral resolution, makes IKONOS images an excellent data source for automated classifications and change detection (Haverkamp and Poulsen, 2003).

A 1-meter true color composite IKONOS product was selected for this research because it offers superior spatial resolution, while retaining the spectral information available in the true color bands. It was produced by a pan-sharpening process with the panchromatic band. The IKONOS composite was projected in a Universal Transverse Mercator (UTM) projection for zone 53 S and set to the World Geodetic System (WGS) 84 datum. Bands 1, 2, and 3 cover the spectral ranges from 0.445-0.516, 0.506-0.595,

Table 1. Spectral (μm) and spatial (m) characteristics of the IKONOS, ASTER, and Landsat TM and ETM+ images.

IKONOS[1]			**ASTER[2]**			**Landsat 5 (TM) and 7 (ETM)[3]**		
Band	Spectral Resolution	Spatial Resolution	Band	Spectral Resolution	Spatial Resolution	Band	Spectral Resolution	Spatial Resolution
1	0.445-0.516	4				1	0.45-0.52	30
2	0.506-0.595	4	1	0.52-0.60	15	2	0.52-0.60	30
3	0.632-0.698	4	2	0.63-0.69	15	3	0.63-0.69	30
4	0.757-0.853	4	3	0.76-0.86	15	4	0.76-0.90	30
			4	1.60-1.70	30	5	1.55-1.75	30
			5	2.145-2.185	30	7	2.08-2.35	30
			6	2.185-2.225	30			
			7	2.235-2.285	30			
			8	2.295-2.365	30			
			9	2.360-2.430	30			
			10	8.125-8.475	90			
			11	8.475-8.825	90			
			12	8.925-9.275	90			
			13	10.25-10.95	90	6	10.4-12.5	60*/120**
			14	10.95-11.65	90			
Panchromatic	0.526-0.929	1				Panchromatic**	0.50-0.90	15

Data obtained from [1] GeoEye (2006). [2] NASA (2006a). [3] NASA (2006c). *Landsat TM data. ** Landsat ETM+ data.

and 0.632-0.698 micrometers, respectively.

4.2. Advanced Spaceborne Thermal Emission and Reflection Radiometer (ASTER) Images

The ASTER sensor was launched in 1999 and began disseminating data to the public in 2000 (ERSDAC, 2006). The sensor is in a sun-synchronous orbit around the earth acquiring images at approximately 10:30 am over the equator. This sensor can image the same geographic location every 16 days and collects data in fourteen spectral bands using three separate radiometers: a Visible Near Infrared (VNIR) radiometer, a Short-wave Infrared (SWIR) radiometer, and a Thermal Infrared (TIR) radiometer collecting data in four, five, and five bands, respectively. The spectral range of each radiometer is of 0.56-0.86, 1.60-2.43, and 8.125-11.65 micrometers and the spatial resolution is 15 m, 30 m, and 90 m, respectively (Table 1). Radiometric resolutions are 8 bits for the VNIR and SWIR radiometers and 12 bits for the TIR radiometer (ERSDAC, 2006).

ASTER data are available at NASA's Land Processes Distributed Active Archive Center (NASA, 2006b). For this thesis, ASTER's Level 1B product was used because it is the lowest level product with geometric and radiometric coefficient corrections applied and can be obtained projected to the UTM, zone 53 S projection and WGS84 datum.

4.3. Landsat TM and ETM+ Images

Landsat data, pertinent to this thesis, were acquired by the Landsat Thematic Mapper (TM) and Enhanced Thematic Mapper (ETM+) sensors, which are carried aboard the

Landsat 5 and Landsat 7 satellites launched in 1984 and 1999, respectively. Both sensors collect data in seven bands. The first five bands and the seventh band spectrally range from 0.45 to 2.35 micrometers, are quantized at 8 bits, and have spatial resolutions of 28.5 m (Table 1). Band 6 records thermal emissions received at the sensor from the earth's surface and has a resolution of 120 m and 60 m for the TM and ETM+ sensors, respectively. The ETM+ sensor has an additional panchromatic band, ranging spectrally from 0.50 to 0.90 micrometers at a spatial resolution of 15 m. The Landsat TM and ETM+ sensors are on orbital paths crossing over the equator between 10:00 and 10:30 a.m. local time and are capable of imaging the same geographic location every 16 days.

For this thesis, level 1G products were ordered from the USGS's Earth Resources Observation and Science (EROS) Internet site (USGS, 2006). These products are geometrically and radiometrically corrected, as well as projected in a UTM projection for zone 53 S and set to the WGS84 datum.

4.4. Topography of the Mt. Jaya Glacier Area

In 2005, the topography of the Mt. Jaya area was derived using Shuttle Radar Topography Mission data (SRTM) (Fig. 3) (Klein and Kincaid, 2006). Elevations acquired from the SRTM data in the areas of the Carstensz glacier and the W. Northwall Firn were quite good and compared well with those obtained in the 1972 survey of the area. However, a large number of missing values in the SRTM dataset existed within the area of the eastern portion of the E. Northwall Firn and, thus, required a great deal of interpolation. A determination of the accuracy of the interpolations in the E. Northwall Firn is difficult as a result of the unreliability of the mapping in 1972 of this same area.

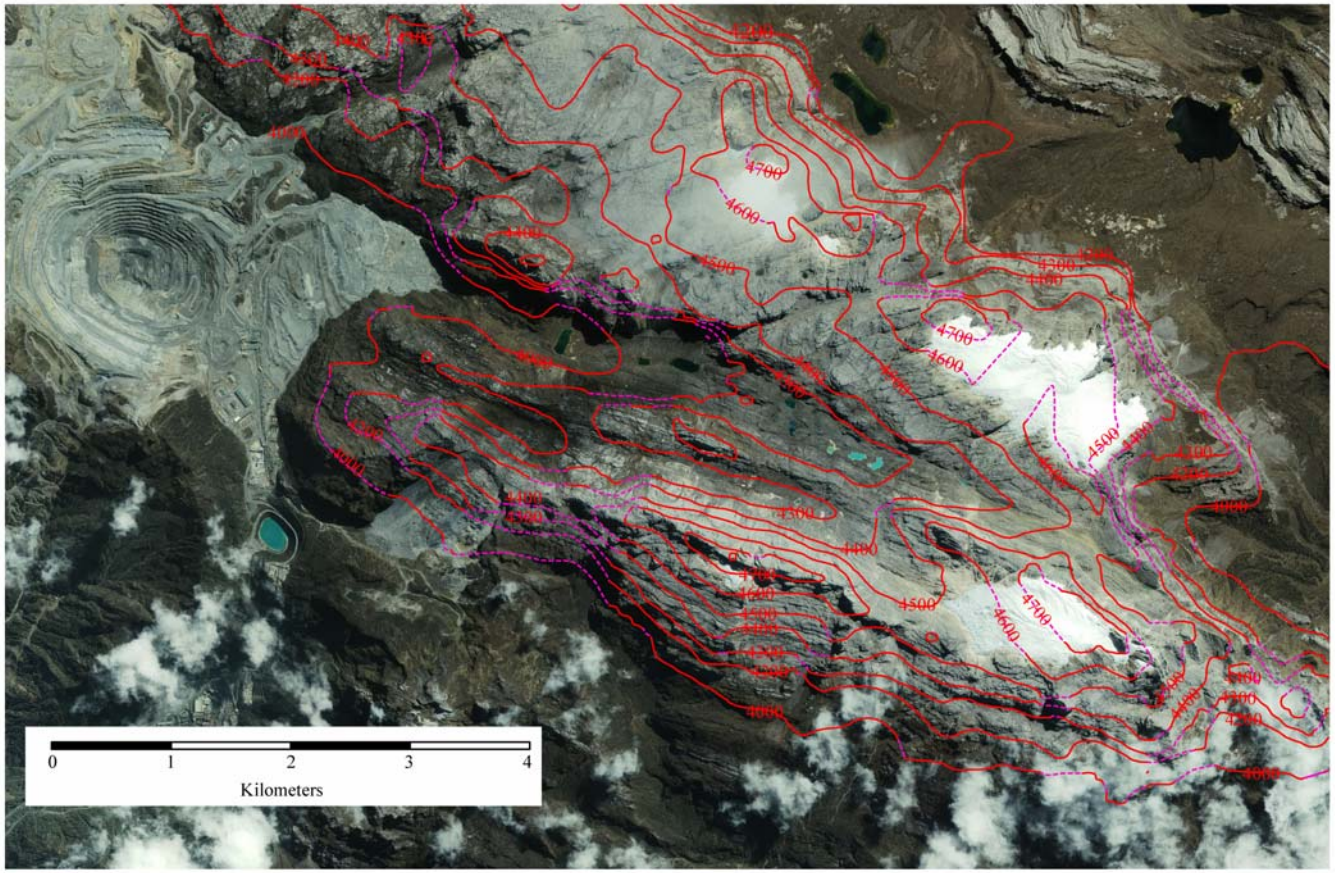

Fig. 3. Topography of the Mt. Jaya area. Topography was derived from SRTM data. Base image is an IKONOS image acquired by the sensor on June 11, 2002. Dotted lines represent areas in which data values were missing from the SRTM data. Map modified from Klein and Kincaid (2006).

However, the topography generated from the SRTM data set should be sufficient to make some general determinations regarding recession of this firn field as the area in question is along the higher reaches of the field.

4.5. National Centers for Environmental Prediction/National Center for Atmospheric Research (NCEP/NCAR) Reanalysis Data

The National Centers for Environmental Prediction/National Center for Atmospheric Research (NCEP/NCAR) Reanalysis data is a modeled 4-dimensional gridded climate data set extending from 1948 to present. The values for meteorological variables used in producing this climate set are acquired from a multitude of sources, including land surface observations, observations from ships, rawinsonde, pibal, aircraft, geostationary satellites, and other sources. The primary purpose for creating this source of climate data was to provide an accurate consistent database for researchers. Atmospheric temperature and pressure height at the 500 hPa level, and atmospheric temperature, pressure height, specific humidity, and wind magnitude at the 600 hPa level, as well as accumulated precipitation, radiation, and percent cloud cover data at the surface were acquired from the NCEP/NCAR Reanalysis dataset at the National Oceanic and Atmospheric Administration (NOAA)-Cooperative Institute for Research in Environmental Sciences (CIRES) website (NOAA-CIRES, 2006). While the values for precipitation and radiation are surface data that are completely derived by the model, the values are forced to closely approximate real observations. The surface dataset has been found to be reliable for seasonal and interannual studies and, therefore, should be appropriate for broad scale purposes here.

While the density of observations is good for the Northern Hemisphere in the earlier years, the quality of modeled results for some areas of the southern hemisphere is limited due to a dearth of observations. However, improvements in data density in the southern hemisphere occurred with increased synoptic land surface reports in the 1950s, in the 1960s with increased ship, radiosonde, and aircraft reports, and in the 1970s with satellite observations. Despite the lower data densities existing in the southern hemisphere, studies indicate that the difference in quality between the northern and southern hemisphere modeling results in the early years is not as significant as would be indicated by the data density reports.

4.6. Oceanic Niño Index (ONI)

Monthly classifications of ENSO events from 1951 to 2005 were acquired from NOAA's National Weather Service's Climate Prediction Center (CPC) (NOAA-CIRES, 2006). Classifications are based on 3-month running means of the extended reconstructed sea surface temperature anomalies in the Niño 3.4 region (5°N-5°S, 120°-170°W). A month is classified as cold or warm based on whether or not a threshold of +/- 0.5°C is met during five consecutive seasons.

4.7. Historical Data

Over the past century, a variety of data sources and methods have been used to measure the area extents of the Mt. Jaya glaciers. As technologies have improved, errors have been discovered and corrections have been made to the originally published glacier

areas. It is prudent to provide a history of the published research because one of the objectives of this thesis is to compare the glacier surface areas over various time periods.

4.7.1. Glacier Extents From ca. 1850-1972

According to Mercer (1967), the only surface area measurements for the Mt. Jaya glaciers published prior to his report for the American Geographical Society had been acquired by Dozy and Colijn in 1936 (Dozy, 1938). Wollaston (1914) only provided a record for the snowline in the area, as he only reached the hanging glaciers on the south face before having to turn back. The Harrer climbing expedition team sought out the cairns previously established by the Dozy team, but were only able to locate the cairn for the Meren glacier (Harrer, 1965). Before leaving the area they constructed new cairns which identify the 1962 ice front for the Meren glacier.

The glacier surface areas on Mt. Jaya in 1913, 1936, 1942, 1962 and1972 were all published by the Australian Universities' team (Allison, 1974; Allison and Peterson, 1989) and ice fronts for each year, as well as the entire glacier boundaries for 1972, are illustrated in the team's 1972 map of the Mt. Jaya area. The 1972 glacier boundaries were determined primarily from field work, and vertical and oblique aerial photographs acquired by the United States Air Force in 1942.

The methods used for delineating various segments of the glacier boundaries are identified on their map. Fieldwork primarily focused on the Carstensz and Meren glacier tongues and the boundaries mapped for these areas are considered the most accurate. A combination of survey and photogrammetric techniques were utilized to map the northern border of the Carstensz, the southwest border of the E. Northwall Firn, and the

entire W. Northwall Firn. However, defining the limits of the W. Northwall Firn was somewhat problematic due to cloud cover in the photos. The eastern-most boundaries of the Carstensz glacier, Meren glacier, and E. Northwall Firn, as well as the southern boundaries of the Meren glacier and a portion of the southern boundary of the Carstensz glacier which includes the Wollaston and Van de Water glaciers were mapped solely from aerial photography after the expedition and the reliability of these glacier boundaries is considered poor (Allison, 1974). Various degrees of uncertainty are associated with each method and clearly defined in the map.

Whereas the 1972 measurements were made in the field, the 1913, 1936, 1942, and 1962 measurements were derived using photographs acquired during each of the visits to the area, cairns that had been established during both the Dozy and Harrer trips, and vertical aerial photographs taken of the area by the United States Air Force in 1942 (Allison, 1974). Photographs supplied by Dozy to the universities and plotted onto the 1972 base map resulted in slightly different area measurements reducing the total glacier area on Mt. Jaya in 1936 from 14.5 km^2 (Mercer, 1967) to 13 km^2 (Allison, 1974; Allison and Peterson, 1976).

Area measurements for ca. 1850 were determined from geomorphic evidence acquired in the field (Peterson and others, 1973). Average retreat rates were calculated at 33 m yr^{-1} and 16 m yr^{-1} for the Meren and Carstensz glaciers, respectively, and extrapolation of these rates suggests that the current recession may have begun about 1820-1850 A.D. (Peterson and others, 1973).

4.7.2. Glacier Extents From 1972-1987

The 1974 area values were measured by Allison and Peterson (1989) from a Landsat Multispectral Scanner (MSS) image. The spatial resolution of Landsat MSS images is 79 m, and therefore, the minimal mapping unit for these images is approximately 6241 m for linear features (Jensen, 2000). Whereas the spatial resolution of Landsat MSS may be limiting, the authors did have first-hand knowledge of the glaciers as both were involved in the 1972 field expeditions and the glaciers were much larger than they are presently. However, the image did afford a larger perspective of the area and it was realized that the eastern boundaries for the 1972 glacier boundaries were incorrect, as were the western boundaries for the E. Northwall Firn. Corrections to these boundaries resulted in raising the original 1972 ice surface areas for the E. Northwall Firn and Carstensz glacier by approximately 0.25 km^2 and 0.2 km^2, respectively.

Allison and Peterson (1989) also analyzed 1982 and 1983 Landsat MSS images of the Mt. Jaya area. The results from their analyses of these images indicated that the glaciers had not changed significantly in extent since 1974, with no more than 100 m of retreat occurring between the time periods. Surface ice areas for the 1982 and 1983 years were not published.

Glacier extents were also measured from a 1987 SPOT image of the area by Peterson and Peterson (1994). SPOT images are of high spatial quality at 20 m resolution. Their data collection and analysis also included a short field visit to the area in 1992. Results of their mapping will be discussed in the next section, as their mapping was used extensively in this thesis.

Peterson and Peterson (1994) published an updated version of the 1972 map produced in the field during the Australian Universities expeditions. They accomplished this by creating a single digital database that included the mapped glacier areas for 1972 and 1987, along with markers for ground control points that were obtained during the 1972 field expeditions. Their mapping confirmed large errors made in the 1972 mapping of the E. Northwall Firn and Carstensz glacier.

5. METHODS

5.1. Acquisition of Satellite Images

A thorough search of Internet sites providing satellite images was completed to identify suitable images for this thesis. To meet the objectives of this thesis the images selected had a clear view of all of the Mt. Jaya glaciers, and a spatial resolution sufficient for detecting small ice masses. According to Jensen (2000), in order to detect landscape features within satellite images the feature must be at least twice the size of a pixel and the spectral resolution of the image must be high enough to discriminate the object from its background. Applying these criteria for identifying suitable images resulted in the acquisition of six images: two IKONOS, one ASTER, one Landsat ETM+, and two Landsat TM images dated 8 June 2000, 11 June 2002, 29 May 2003, 29 May 2003, 26 July 2004, and 11 June 2005, respectively (Figs. 4-9). Unfortunately, there were not any remotely sensed images acquired in 2001 that were deemed suitable for this thesis.

Applying Jensen's requirements for feature detection within remotely sensed images, the spatial resolutions of the IKONOS, ASTER, and Landsat data enable a minimum mapping unit of 16, 900 m^2 and 800 m^2 in surface area, respectively. Investigation into the area requirements for inclusion into the World Glacier Monitoring Service database indicates that glaciers must measure at least >0.001 km^2 (i.e. 1000 m^2) when utilizing remotely sensed images to attain the measurement. However, historically, ice masses less than 0.1 km^2 (i.e. 100,000 m^2) were not included in the overall totals of glacier ice for Mt. Jaya (Allison, 1974; Allison and Peterson, 1976). Therefore, the sensor data acquired for this thesis should be sufficient for detecting the Mt. Jaya glaciers.

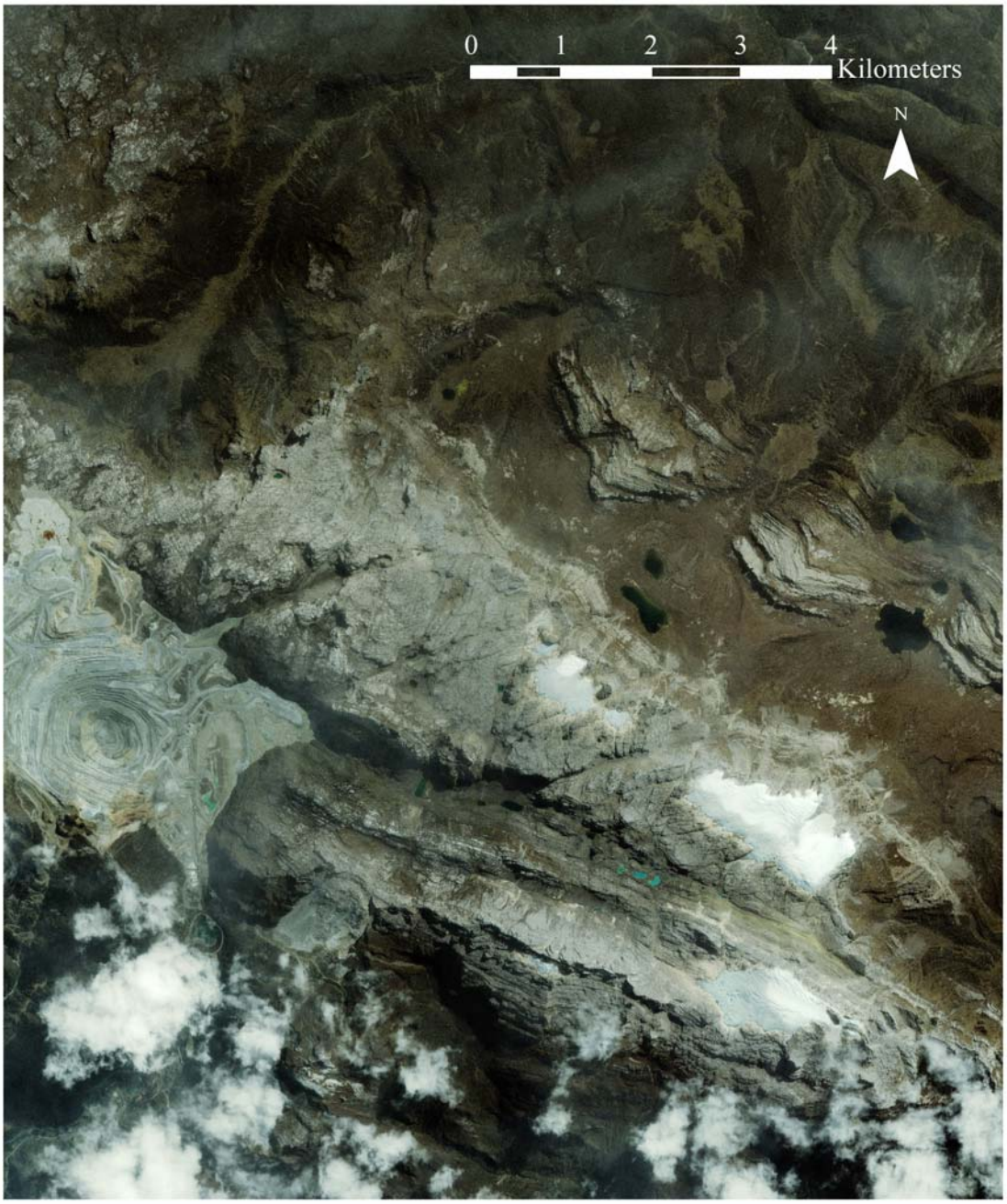

Fig. 4. Original 2000 IKONOS image of the Mt. Jaya glaciers. This 1-meter true color image was acquired by the sensor on June 08, 2000. Geographic datum: WGS84, Coordinate System: UTM 53S.

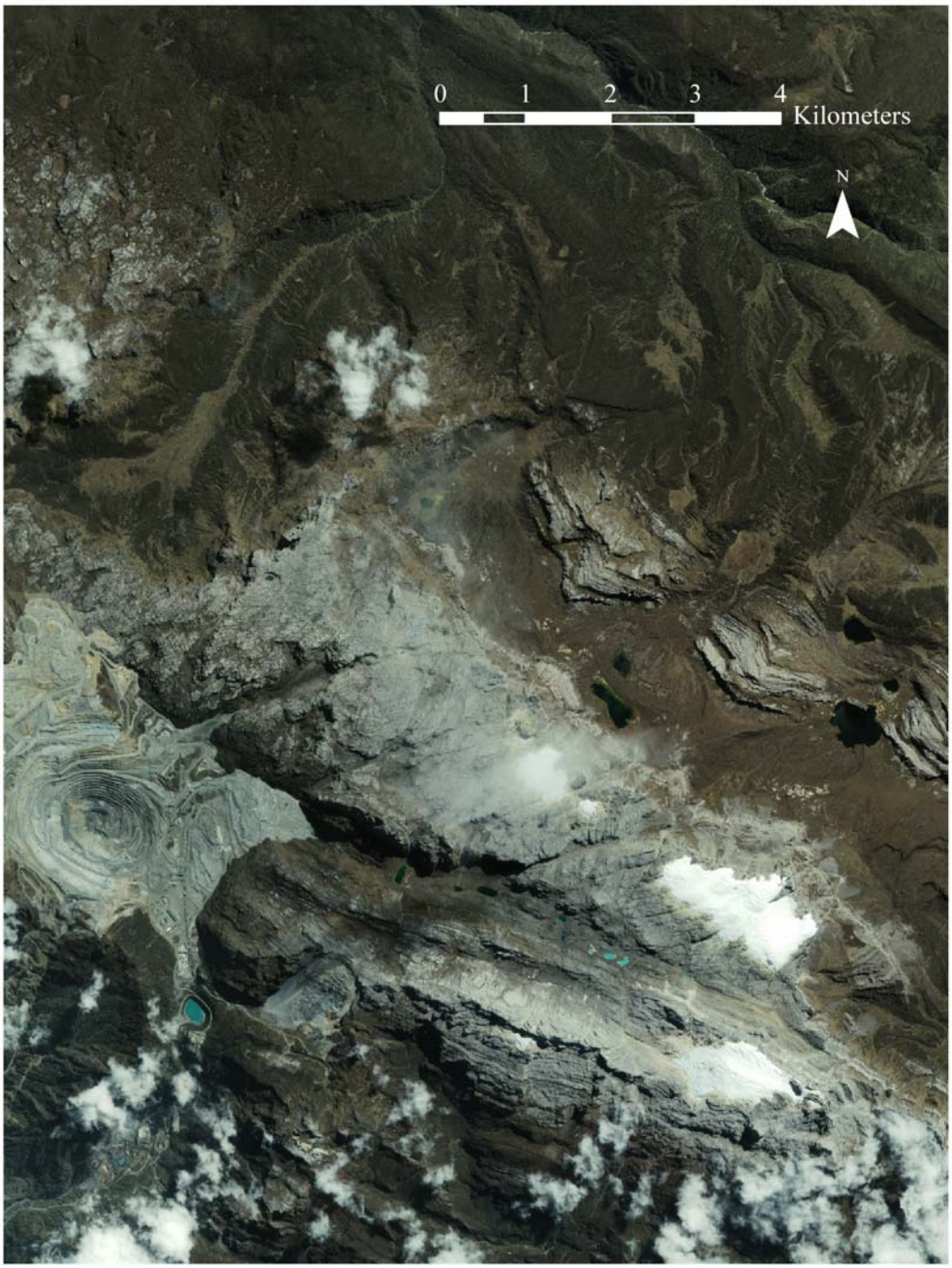

Fig. 5. Original 2002 IKONOS image of the Mt. Jaya glaciers. This 1-meter true color image was acquired by the sensor on June 11, 2002. Geographic datum: WGS84, Coordinate System: UTM 53S.

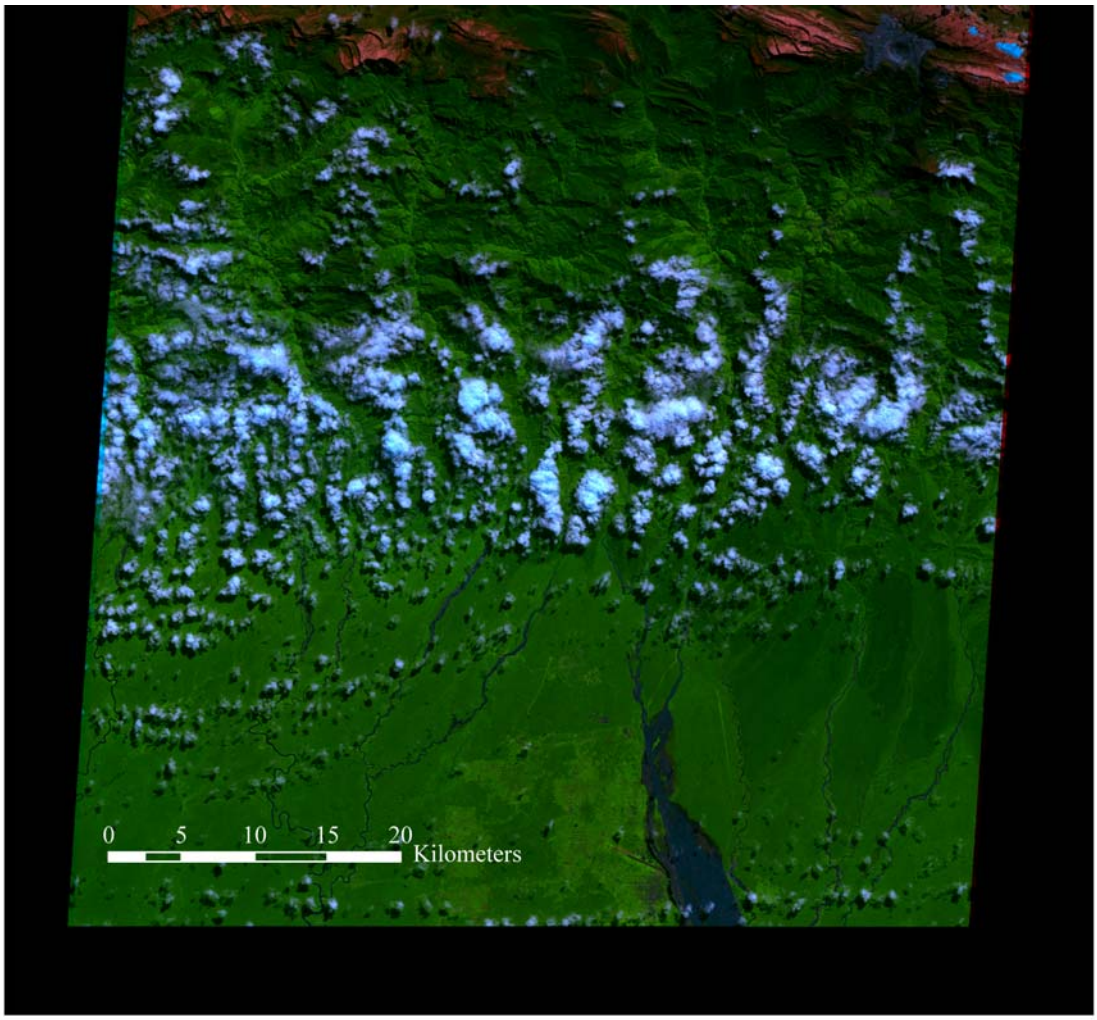

Fig. 6. Original 2003 ASTER image of the Mt. Jaya glaciers. This 15-meter image was acquired by the sensor on May 29, 2003. Geographic datum: WGS84, Coordinate System: UTM 53S, RGB=432.

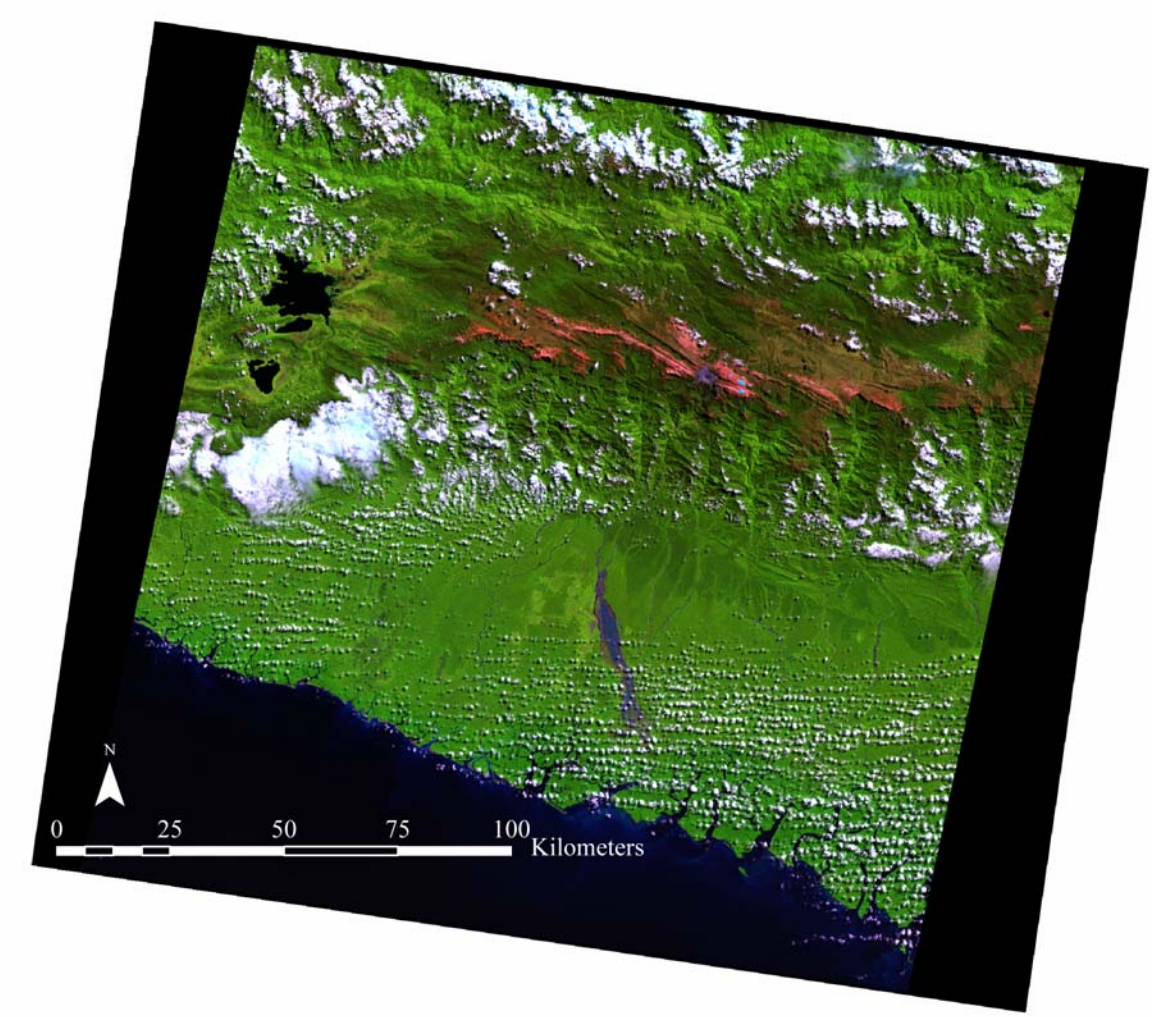

Fig. 7. Original 2003 Landsat ETM+ image of the Mt. Jaya glaciers. This 28.5-meter image was acquired by the sensor on May 29, 2003. Geographic datum: WGS84, Coordinate System: UTM 53S, RGB=543.

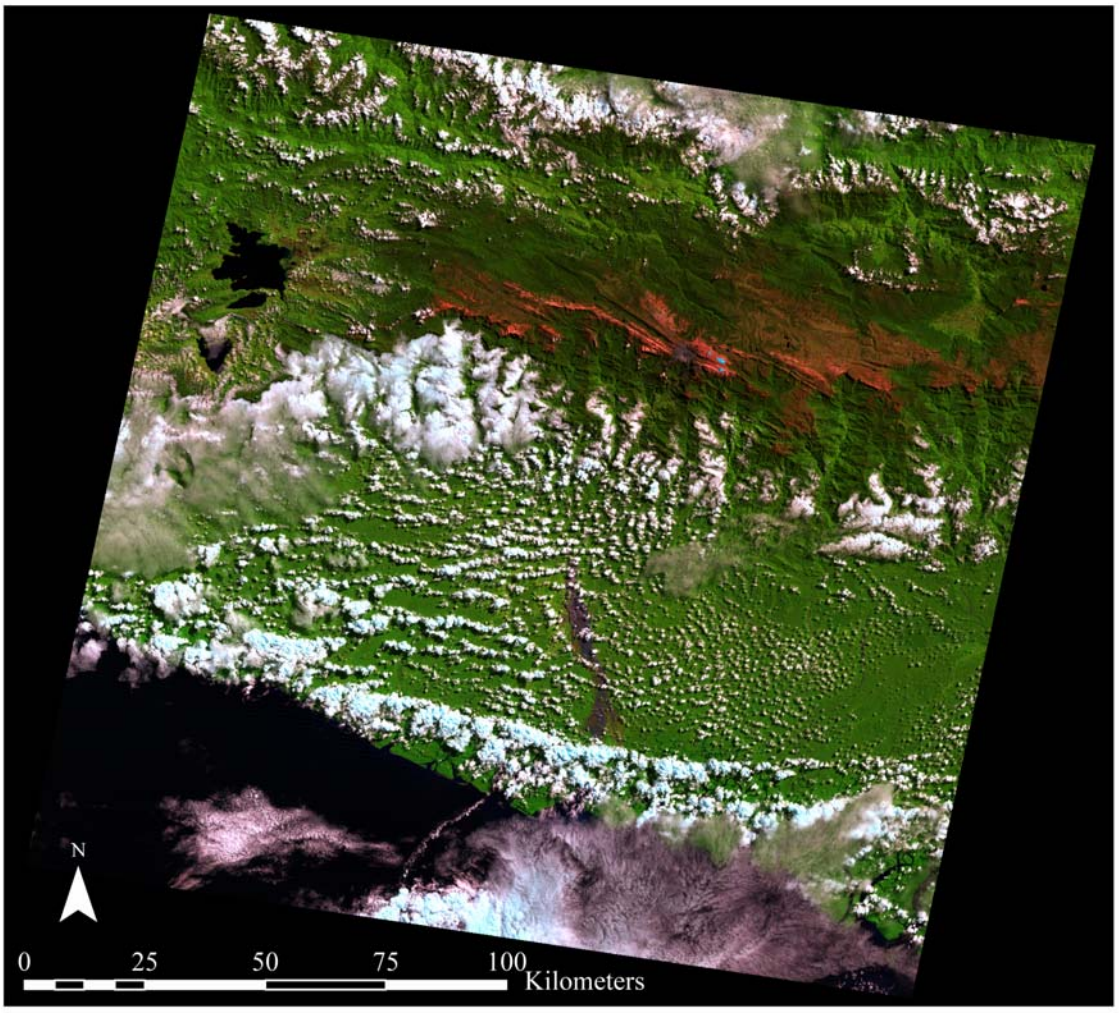

Fig. 8. Original 2004 Landsat TM image of the Mt. Jaya glaciers. This 28.5-meter image was acquired by the sensor on July 26, 2004. Geographic datum: WGS84, Coordinate System: UTM 53S, RGB=543.

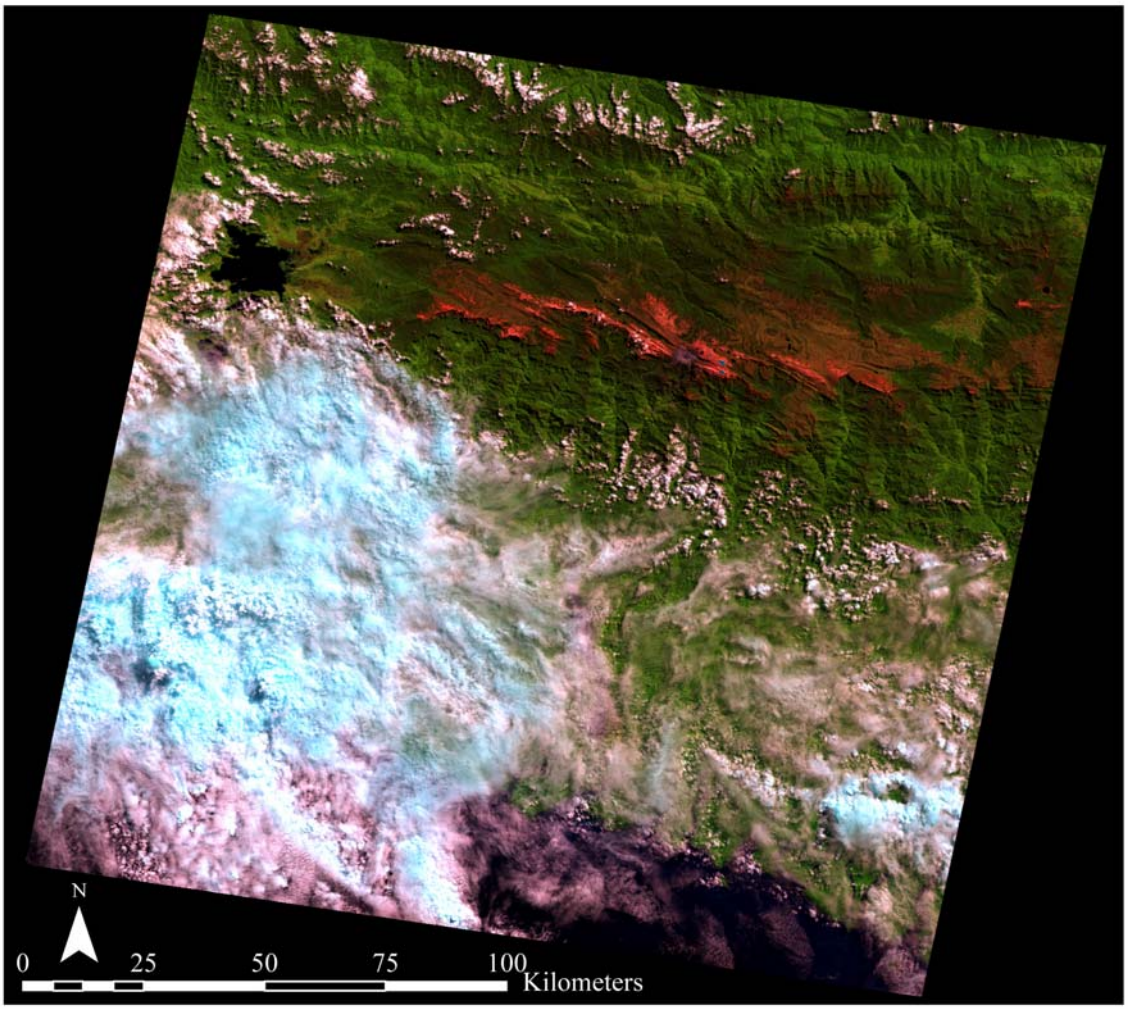

Fig. 9. Original 2005 Landsat TM image of the Mt. Jaya glaciers. This 28.5-meter image was acquired by the sensor on June 11, 2005. Geographic datum: WGS84, Coordinate System: UTM 53S, RGB=543.

Spectrally, the interface between ice/snow and the surrounding bedrock are clearly visible within all of the images.

The actual dates selected for analysis were determined primarily by the availability of cloud-free images. Although seasonal differences on tropical glaciers are not considered to be great, studies on the inner tropical glacier Antizana 15 indicate that small seasonal changes in some climate variables do occur and can affect glacier processes (Favier and others, 2004a; Francou and others, 2004). Therefore, it is advantageous to this thesis that all images were acquired during May-July time periods so that seasonal differences on the glaciers will less likely complicate comparisons of climate and glacier changes.

5.2. Preprocessing Satellite Images: Band Selection for Color Composites

The IKONOS data product was delivered as a true color composite and therefore, band selection was not necessary. Band composites that would highlight the glacier/rock interfaces had to be created for the ASTER and Landsat images. After experimenting with several band combinations and visually examining the results it was determined that bands 4, 3, and 2 and bands 5, 4, and 3 for the ASTER and Landsat composites, respectively, resulted in the best highlighting of the glacier/rock interface. Figures 10 and 11 illustrate the contrast at the glacier/rock boundary on the IKONOS images, and the Landsat and ASTER composites, respectively. Table 1 illustrates the correspondence between the selected bands.

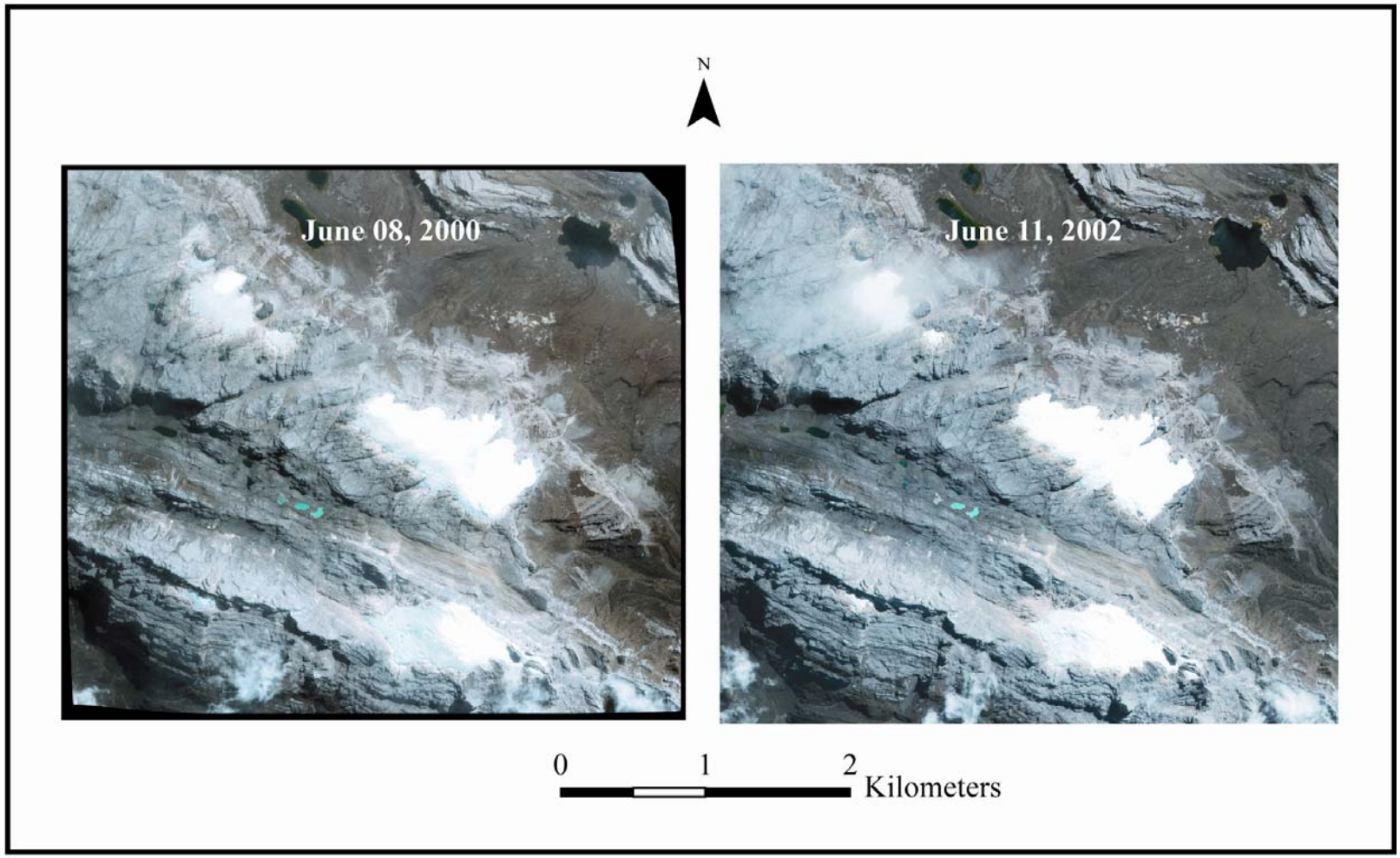

Fig. 10. Subsets of the IKONOS images after processing. The 2000 and 2002 images are true color images and have 1 m spatial resolutions as a result of pan-sharpening.

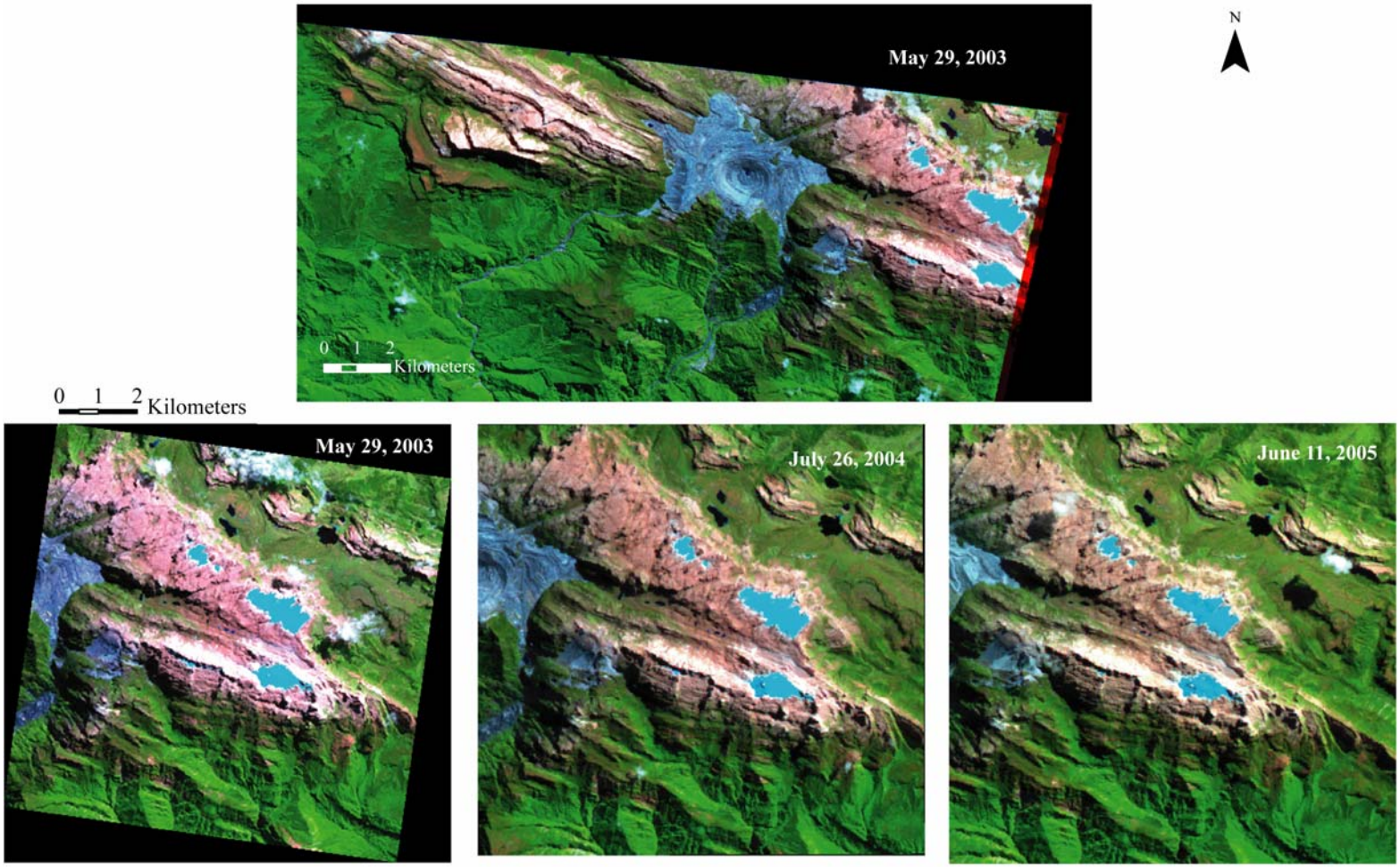

Fig. 11. Subsets of the coregistered ASTER and Landsat composites. The 2003 ASTER image (above) has a spatial resolution of 15 m and consists of a 432=RGB color composite. The Landsat scenes (below) have spatial resolutions of 28.5 m and each consist of a 543=RGB color composite. These images illustrate how clearly the glacier/rock boundary can be seen in the images.

As Table 1 illustrates, band 4 of the ASTER data has a spatial resolution of 30 m, whereas bands 2 and 3 are 15 m. To create the 432 band composite for the ASTER image, band 4 was resampled to 15 m by nearest neighbor interpolation. Therefore, the accuracy of glacier mapping from the ASTER 432 composite is limited to 30 m.

5.3. Coregistration of the Satellite Images

5.3.1. IKONOS Images

To facilitate the visual detection of surface ice area changes that occurred between 2000 and 2002 the IKONOS images were co-registered. The image-to-image registration was first attempted using a global polynomial transformation. This process entails selecting common points found in both images and then applying a polynomial transformation to the target image which results in warping the image so that the geolocation of each pixel corresponds with the pixels in the base image. The calculation for the transformation can be a first order polynomial which requires as few as three ground control points (GCPs) or higher order polynomials can be utilized. The use of higher order polynomials requires an increasingly higher number of GCPs with each increase in order. In this case, a third order polynomial using twenty GCPs resulted in the least error. However, a visual inspection of the resulting image deemed it unsatisfactory. Local variations across the image, enhanced by the high spatial resolution of the IKONOS images, seem to be the main cause of this distortion.

To accommodate for the local variations, subsets of the images were created of the area of interest and an automated cross correlation routine was implemented resulting in the identification of over 25,000 GCPs. The root mean square (RMS) error calculated by

the program code was less than 1 m. Once the GCPs had been identified, Delaunay triangulation transformation was applied for final rectification of the target image. Errors of approximately 1 m were identified for approximately 95% of the image through a visual inspection. A few small areas of high relief and shadowing complicated the procedure and errors as high as 8 m were observed.

5.3.2. ASTER Image

Consistent with the coregistration of the IKONOS images, the 2003 ASTER image was georeferenced to the 2002 IKONOS image. A first order global polynomial transformation resulted in an RMS error of 0.66 pixels. This implies that for each point utilized to warp the image, the average displacement of the point in the warped image from its original position was 0.66 pixels (i.e. approximately 20 m). A visual inspection indicated that the transformation was successful over most of the image. However, some areas, primarily around the small portion of the tail of the Carstensz, were off by approximately 40 m. This was not surprising because not only was the tail of the Carstensz glacier located along the periphery of the image, but this area is also one of very diverse relief.

5.3.3. Landsat TM and ETM+ Images

The Landsat images were subset to areas comparable to those created with the IKONOS images. First order global polynomial transformations were applied on the 2003, 2004, and 2005 Landsat subsets, respectively, using the 2002 IKONOS image as the base image. Although all three rectifications resulted in RMS errors of less than 30 m (i.e.

less than one pixel), a visual inspection of the results indicated that unacceptable errors existed when comparing the warped Landsat images. The most likely cause of these errors was the identification of good GCPs within the images. Not only were acceptable GCPs lacking, but the 26 m difference in spatial resolution between the IKONOS (4 m) and Landsat (30 m) images further complicated the procedure. Therefore, the 2004 Landsat image was rectified to the 2002 IKONOS and the 2003 and 2005 Landsat images were rectified to the 2004 Landsat image resulting in RMS errors of 0.479 (13.7 m), 0.319 (9.1 m), and 0.518 (14.8 m), respectively. Although using this method most likely resulted in error propagation, this method resulted in both, acceptable RMS errors and the best visual results. A visual inspection of the 2004 Landsat image after warping it to the 2002 IKONOS indicates that over most of the image the coregistration was successful. In some areas around the W. Northwall Firn and at a rock protrusion within the Carstensz the error appears to be approximately 30 m. The 2003 to 2004 and the 2005 to 2004 transformations visually appear to have been successful over most of the glacierized areas. In a small portion of the images, probably less than 5%, errors of up to approximately 30 m (one pixel) were observed.

5.4. Glacial Boundary Mapping

All surface ice areas were mapped by visual interpretation and manual digitization in a Geographic Information System (GIS).

5.4.1. Mapping from the IKONOS Images

Visual inspections of the 1-meter IKONOS images indicated that it was possible to detect several features within the images including ice, snow, and recently glaciated areas. There was little supraglacial debris and an absence of moraines along the edges, both of which facilitated the mapping process. In general, at the ice/rock interface the digital numbers for the rock were much higher than that for the older ice. Snow cover was restricted to the higher elevations of the glacier where less melt has occurred. Therefore, at the snow/rock interface the snow had much higher reflectance. This variation in digital numbers made it possible to delineate the glacier borders by individual pixels at an approximate scale of 1:1000. There were only a few areas where this was not the case. In these areas, it was necessary to use a 1:4000 scale in order to define the general boundary location. Following the determination of the general boundary, the 1:1000 scale could then again be utilized to more precisely demarcate the ice border. Figures 12 and 13 illustrate the two most difficult areas to accurately map: the ice/rock interface along a small portion of the southern edge of the East Northwall Firn and the snow/rock interface around the Carstensz tail, respectively. Also complicating the mapping around the Carstensz tail was the steep, rugged terrain and shadowing. Overall, these areas were not common and it was possible to maintain mapping errors to ± one meter.

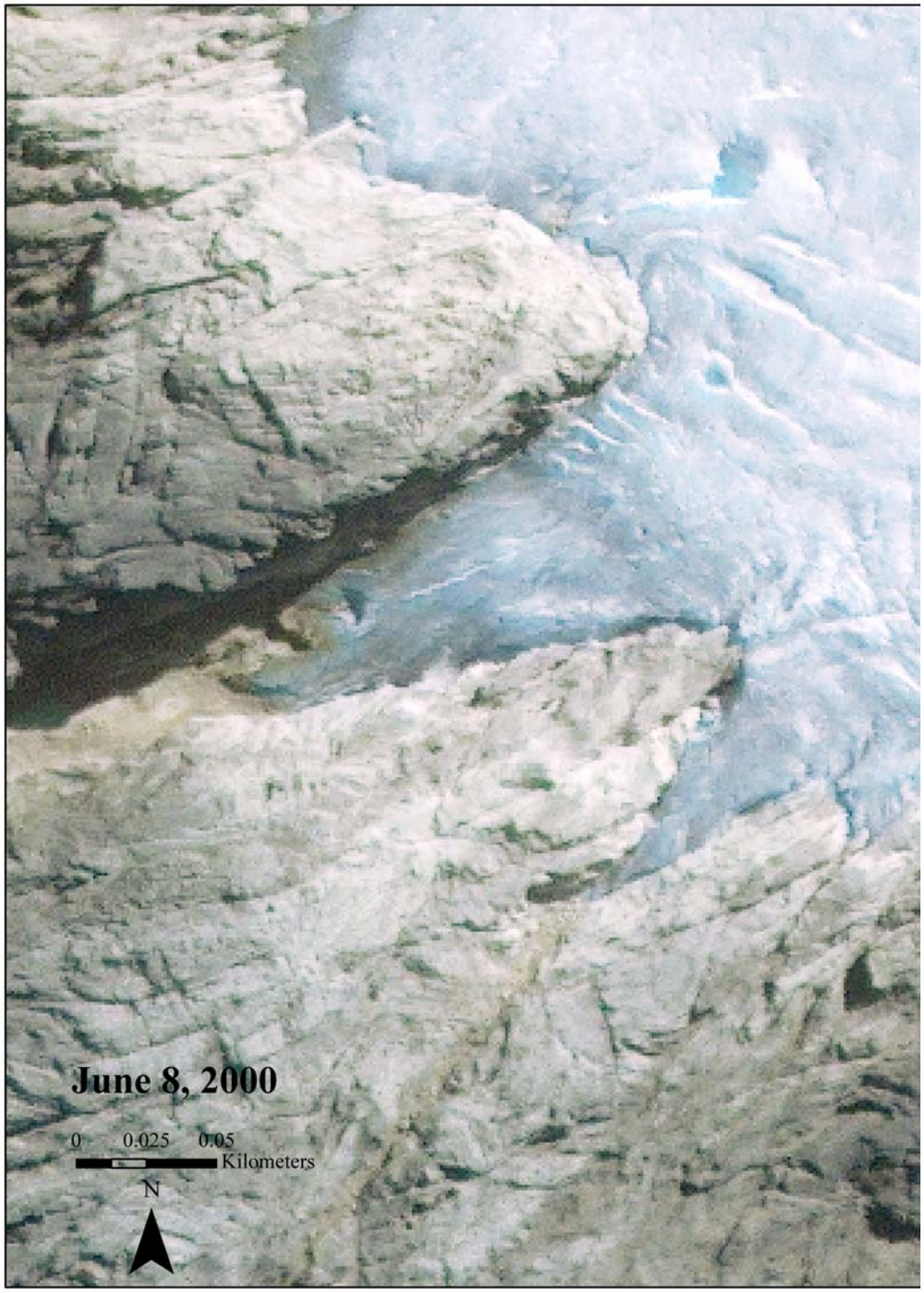

Fig. 12. Distinguishing ice from rock. One of the more difficult areas to visually interpret in the IKONOS image lies along the southern edge of the E. Northwall Firn. The reflectance values for the ice and the surrounding rock are very similar.

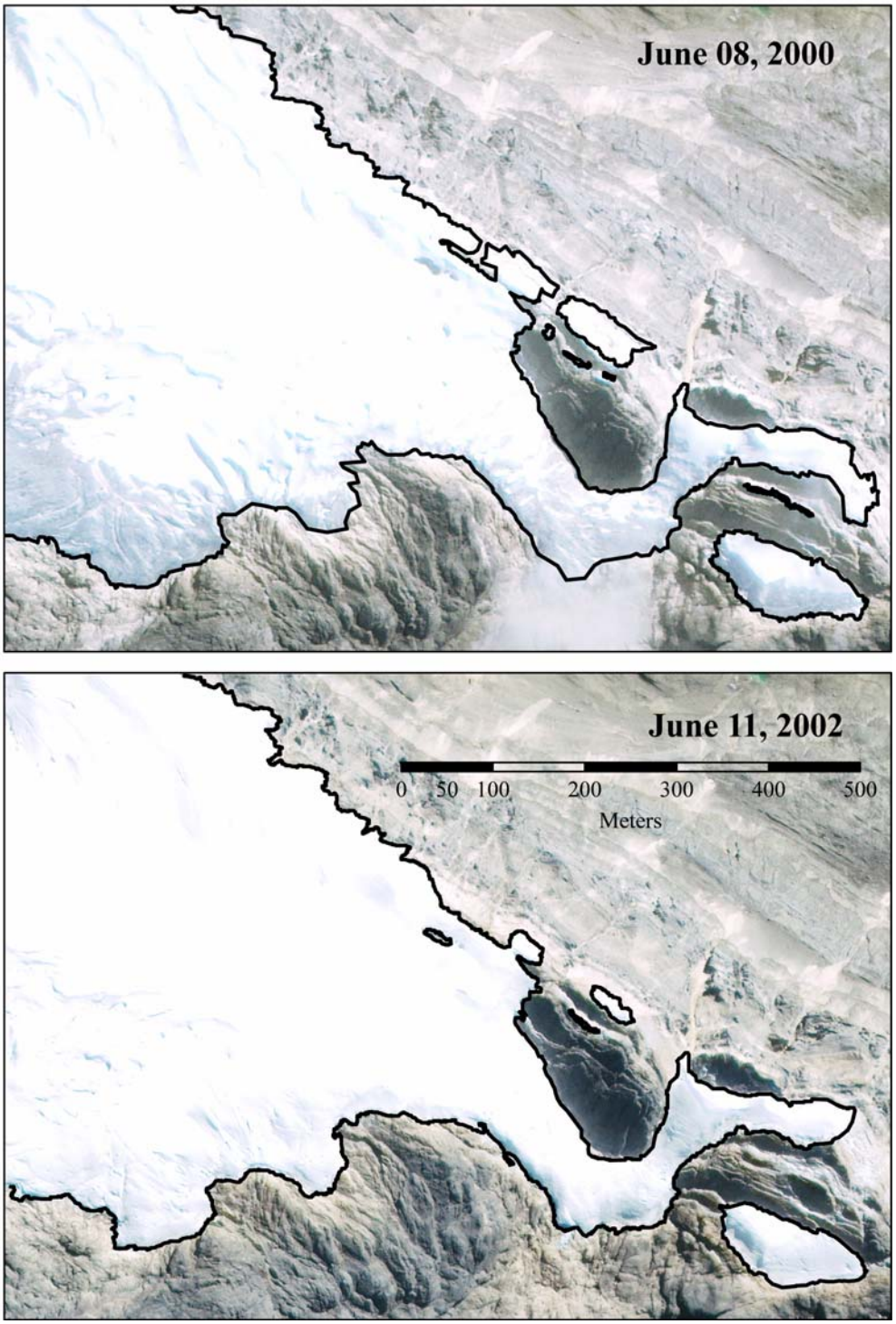

Fig. 13. Mapping the Carstensz tail. Visual interpretation of the snow/rock interface around the Carstensz tail was complicated by steep, rugged terrain, shadowing, and similarities in the reflectance values of the snow and recently glaciated limestone. Map is modified from Klein and Kincaid (2006).

5.4.2. Mapping from the ASTER Image

Despite the lower resolution of the ASTER image, snow and ice were still distinguishable as a result of the high spectral quality of the bands. In addition, as a result of the higher spectral quality of the ASTER image, there was greater contrast between ice/snow and the surrounding rock at the glacier boundaries, thereby facilitating mapping. The same mapping procedure that was used for mapping the IKONOS images was utilized for the ASTER. However, as a result of the lower spatial resolution, delineation of the glacier boundaries was completed at 1:2000 scales. Overall, it was possible to map the boundaries within ± one pixel (i.e. 30 meters).

Unfortunately, only one cloud-free image of the Mt. Jaya glaciers was available from the ASTER archives. Within this image, the glaciers are on the periphery, and a small portion of the Carstensz glacier tail is missing (Fig. 11). To account for the area of the missing tail this portion of the Carstensz was delineated in the 2003 Landsat ETM+ image (mapping of the 2003 ETM+ image is described in section 5.4.3), which was acquired by the sensor on the same day as the ASTER scene, and added to the Carstensz surface area measured from the ASTER image.

5.4.3. Mapping from the Landsat TM and ETM+ Images

The Landsat images were also spectrally superior to the IKONOS images, creating greater contrast at the glacier/rock interface and facilitating mapping. However, it was not possible to distinguish between snow and ice as a result of the broader bandwidths of the Landsat data when compared to the ASTER. The lower spatial resolution of the Landsat and ASTER images also resulted in more difficulties with visually interpreting

mixed pixels. A great deal of effort and care was afforded to maintaining a consistent approach when mapping the glaciers in each of the images. To insure a non-biased approach to the mapping, comparisons between the images were not made during the mapping process. Keeping this in mind, along most of the glacier boundaries delineated in each image, mapping was accomplished within ± one pixel (i.e. 28.5 m).

5.5. Comparing Historical Extents with 2000 to 2005 Surface Areas

To compare glacier surface areas in 1972 and 1987 to those from 2000-2005, the glacier extents provided in the 1972 and 1987 maps had to be digitized in a GIS. Numerous attempts to rectify the 1973 map to the 2002 IKONOS image were unsuccessful. However, it was determined that both the 1973 map and 2002 image could successfully be coregistered to the 1987 map. Therefore, the 1987 map was used as the base image to rectify the 1972 map. This was accomplished using the eleven ground control points that had been established in the field and were marked on both maps. Application of a 1st order (affine) transformation resulted in an RMS error of 1.2 m. The 1973 and 1987 maps, respectively, were then rectified to the 2002 IKONOS subset using ten tie points that were identifiable in both of the maps and the image. These points primarily consisted of glacial lakes and rock formations at the Carstensz top. 1st order transformations were used in both cases and resulted in RMS errors of 37.08 m.

After coregistration, the glaciers were digitized from the 1972 and 1987 maps and overlaid in a GIS. A visual inspection of the resulting map indicated that it closely resembled the results that Peterson and Peterson (1994) obtained. Peterson and Peterson

(1994) did not differentiate the individual glaciers in their analysis. Therefore, as a final step, the 1987 surface areas for each glacier were measured in a GIS.

5.6. Climate Data Analysis

Freezing level was calculated at 6 hour intervals using the temperature and pressure height data at 500 and 600 hPa. This was accomplished by determining the interval in meters existing between these two pressure levels, dividing it by the change in temperature occurring between these two levels, multiplying this result by the degrees necessary to reach 0°C, and adding that result to the 600 hPa pressure height.

The NCAR/NCEP Reanalysis data, along with the freezing level results, were analyzed on a monthly basis for the period 1951-2005 to correspond with the temporal resolution of the ENSO classification acquired from the CPC. To facilitate a broad scale comparison between the changes occurring to the Mt. Jaya glaciers and changes in the meteorological variables, the monthly means (monthly sum in the case of accumulated precipitation) were aggregated into single means to coincide with periods of glacial observations. Periods representing major observations of the glaciers are defined as 1972-1987 and 1988-2005. To provide an indication of climate conditions prior to 1972, the data for 1951-1971 was also aggregated.

To test for the statistical significance in the differences in means between periods for each of the climate variables, t-tests at the 95% confidence level were run. If the significance value of the T-test was less than 0.05 then the variable was considered to have changed from one period to the next, but if the significance value was higher than 0.05 then the mean for the variable was not considered to have changed. In addition to

testing the significance of magnitude changes in the monthly SSTs, frequency of ENSO classifications were calculated to determine if the occurrence of El Niño events had changed between periods.

During each time period, respectively, the monthly means for each climate variable (i.e., atmospheric temperature, freezing level, accumulated precipitation, accumulated convective precipitation, radiation, percent cloud cover, specific humidity, and wind speed) was examined to determine if the pattern of change from period to period was similar to that of the ONI.

6. RESULTS

6.1. 2000 to 2005 Mapping Results

The dramatic recession of the Mt. Jaya glaciers documented since ca. 1850 has continued into the 21st century. Of the seven ice masses documented on Mt. Jaya in 1972 (the E. and W. Northwall Firns, and the Carstensz, Meren, Wollaston, Van de Water, and Southwall Hanging glaciers), only four remain. These include the E. and W. Northwall Firns, the Carstensz, and the Southwall Hanging glacier. The tongue of the Meren glacier and the Middle Firn area are gone. All that remains of the Meren is the portion of the E. Northwall Firn that previously flowed into the glacier. The Wollaston glacier has completely receded and the Van de Water glacier only exists as small, fragmented ice masses. Therefore, any possible remains of these two glaciers are incorporated into the Carstensz glacier area. Figures 14 through 17 illustrate the recession of the remaining glaciers over the 2000-2005 period.

Table 2 provides the surface areas for all of the ice masses mapped from 2000-2005. Two totals for the Mt. Jaya area are provided in the table. The first value represents the total surface ice area for Mt. Jaya including all ice masses >0.001 km^2, as this is the minimum mapping unit now required for standardization by the World Glacier Monitoring Service. These totals were 2.327, 2.153, 1.913, 2.107, 1.936, and 1.728 km^2 for May 2000, June 2002, May 2003 (ASTER), May 2003 (Landsat ETM+), July 2004, and June 2005, respectively. Following protocols established in previous reporting for the Mt. Jaya glaciers, the second value provided in the table represents the total for all

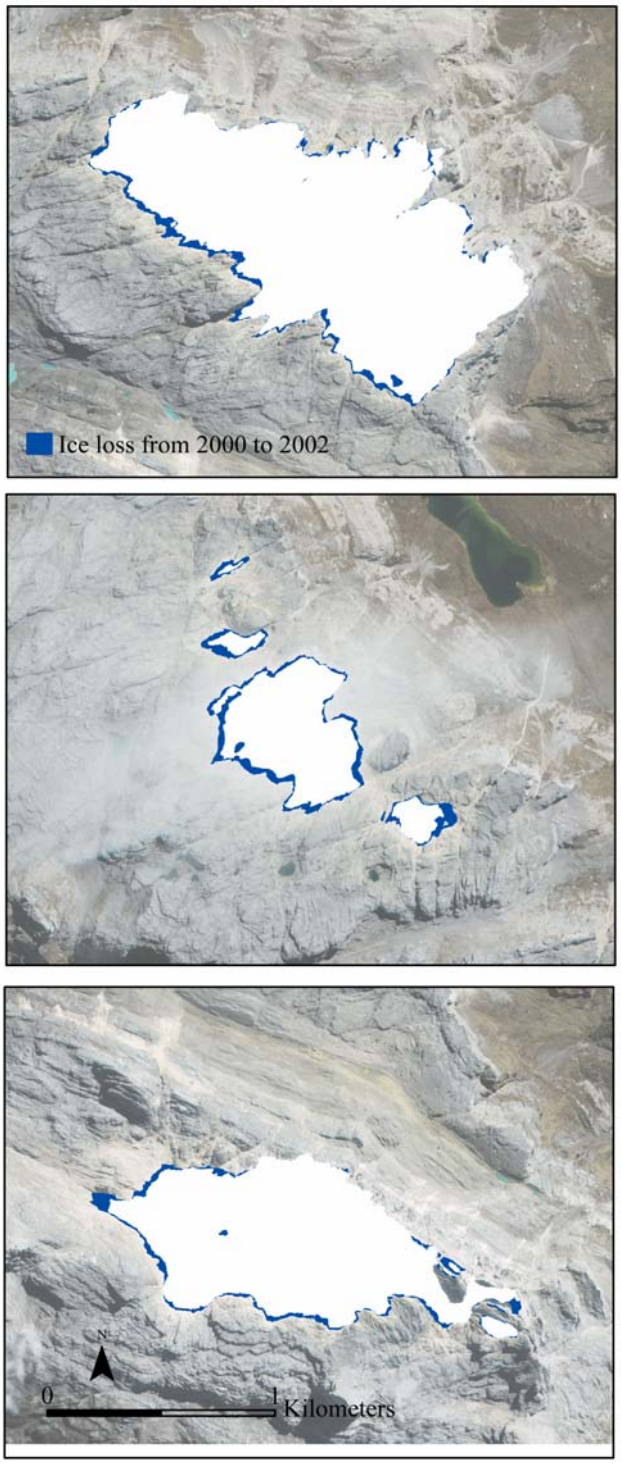

Fig. 14. Ice loss for the Mt. Jaya glaciers from 2000 to 2002. Mapping was accomplished using the 2000 and 2002 IKONOS images. Top: E. Northwall Firn; Center: W. Northwall Firn; Bottom: Carstensz glacier. Maps modified from Klein and Kincaid (2006).

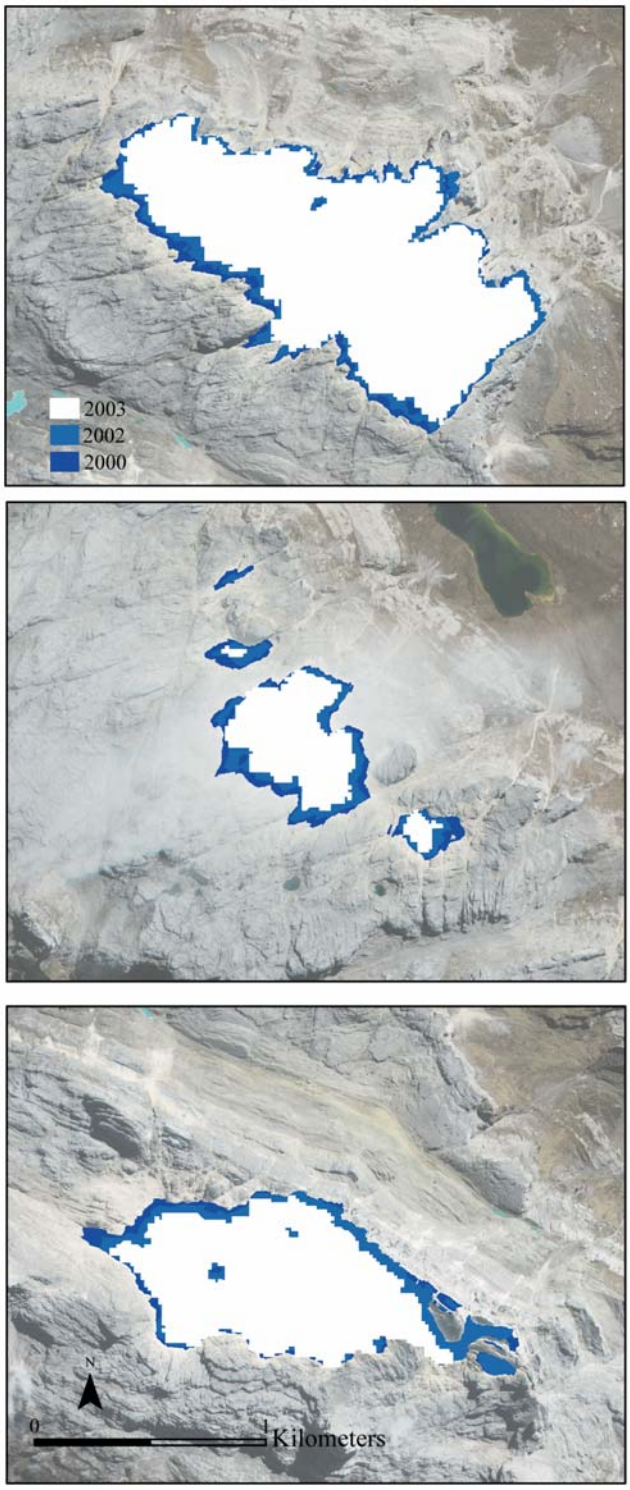

Fig. 15. Ice loss for the Mt. Jaya glaciers from 2000 to 2003. Mapping was accomplished using the 2000 and 2002 IKONOS images and the 2003 ASTER image. Top: E. Northwall Firn; Center: W. Northwall Firn; Bottom: Carstensz glacier.

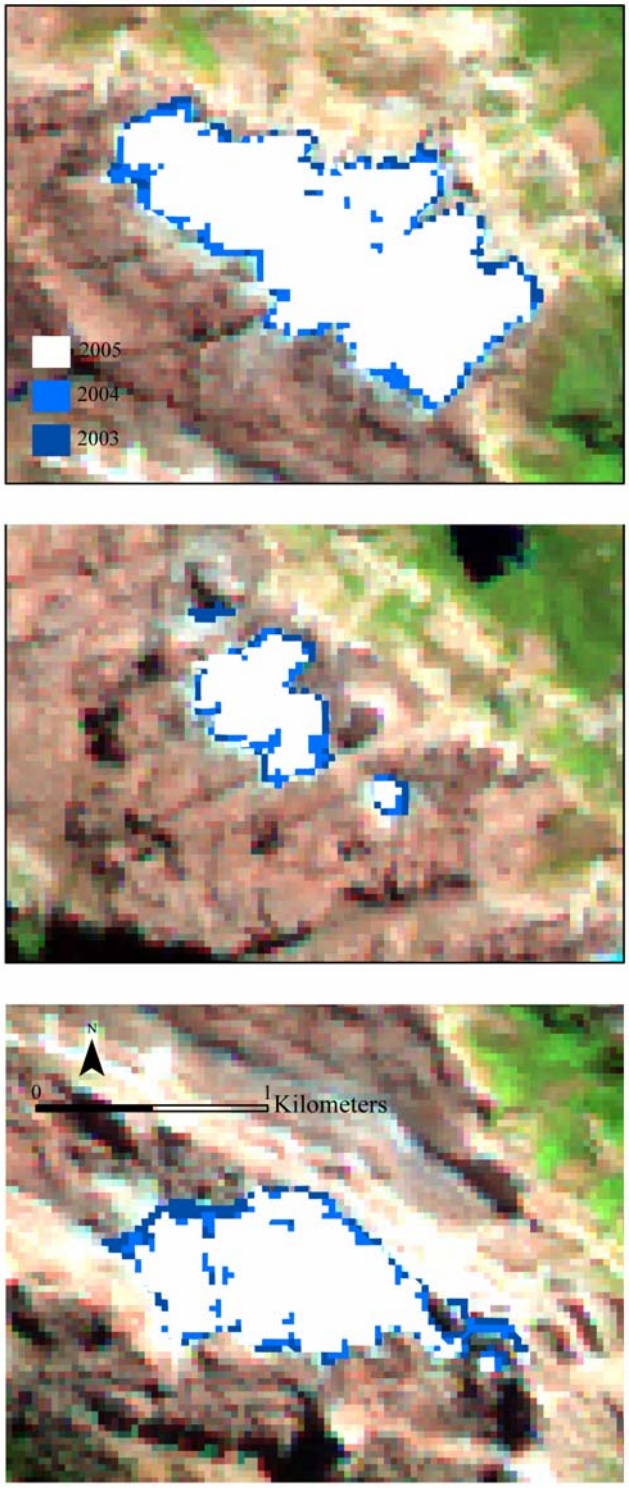

Fig. 16. Ice loss for the Mt. Jaya glaciers from 2003 to 2005. Mapping was accomplished using a 543 color composite created from Landsat ETM+ data. Top: E. Northwall Firn; Center: W. Northwall Firn; Bottom: Carstensz glacier.

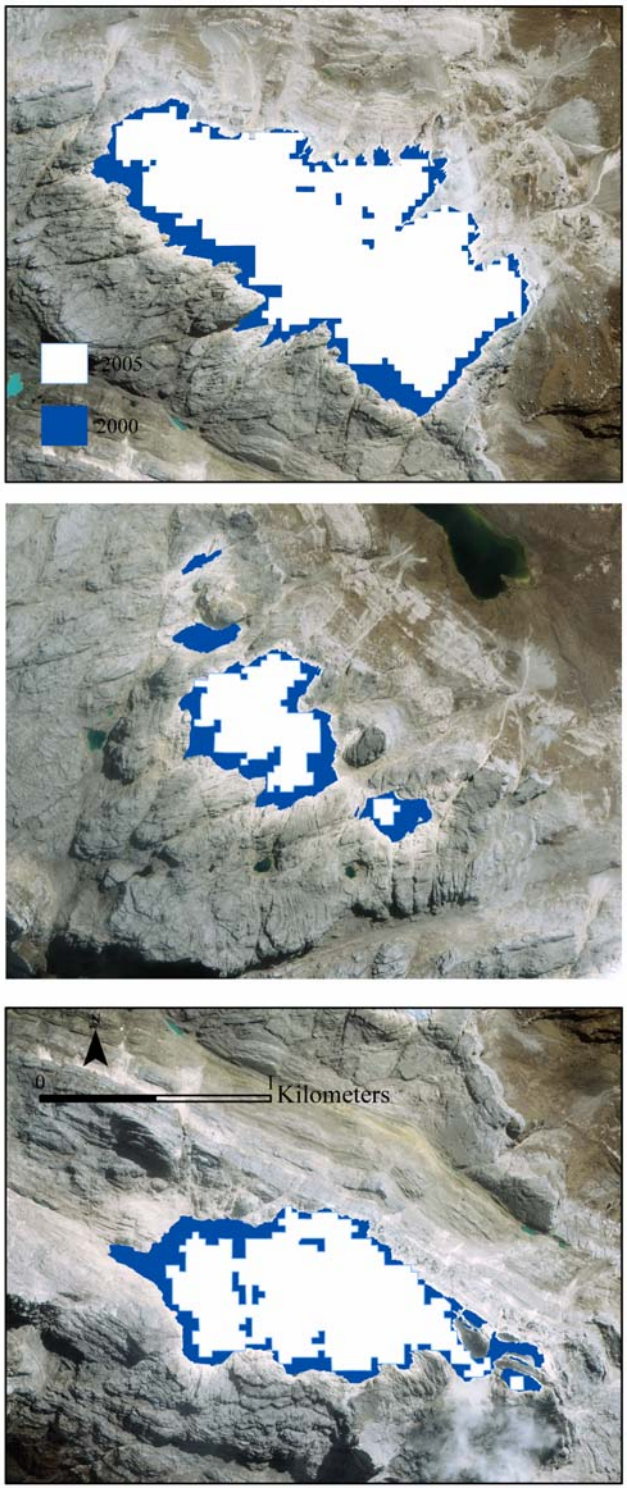

Fig. 17. Ice loss for the Mt. Jaya glaciers from 2000 to 2005. Mapping was accomplished using the 2000 IKONO image and the 2005 Landsat image. Top: E. Northwall Firn; Center: W. Northwall Firn; Bottom: Carstensz glacier.

Table 2. Surface ice areas (km^2) for the Mt. Jaya glaciers from 2000 to 2005.

Glacier	2000 Area[1] (IKONOS)	2002 Area[1] (IKONOS)	2003 Area (ASTER)	2003 Area (Landsat ETM+)	2004 Area (Landsat TM)	2005 Area (Landsat TM)
All Mt. Jaya Glaciers[2]	**2.327** **2.250**	**2.153** **2.101**	**1.913** **1.888**	**2.107** **2.069**	**1.936** **1.908**	**1.728** **1.715**
Carstensz Glacier	**0.747**	**0.696**	**[0.636][3]**	**0.712**	**0.619**	**0.552**
Main Area	0.734	0.686	**[0.629][3]**	0.705	0.612	0.549
Ice Mass 1	0.010	0.009	*	*	*	*
Ice Mass 2	0.003	0.001	[0.007][3]	0.007	0.007	0.003
Ice Mass 3	<0.001	0.000				
Ice Mass 4	<0.001	<0.001	*	*	*	*
Ice Mass 5	<0.001	0.000				
Ice Mass 6	<0.001	0.000				
E. Northwall Firn	**1.228**	**1.173**	**1.061**	**1.120**	**1.084**	**0.982**
Main Area	1.228	1.170	1.061	1.120	1.084	0.982
Ice Mass 1		0.003	*	*	*	*
Ice Mass 2		<0.001	*	*	*	*
W. Northwall Firn	**0.352**	**0.284**	**0.216**	**0.275**	**0.233**	**0.194**
Main Area	0.288	0.245	0.198	0.244	0.212	0.184
Ice Mass 1	0.037	0.026	0.015	0.022	0.015	0.010
Ice Mass 1a	<0.001	0.000				
Ice Mass 2	0.022	0.012	0.003	0.009	0.006	0.000
Ice Mass 3	0.005	0.001	*	*	*	*

Table 2 Continued.

Glacier	2000 Area (IKONOS)[1]	2002 Area (IKONOS)[1]	2003 Area (ASTER)[1]	2003 Area (Landsat ETM+)[1]	2004 Area (Landsat TM)[1]	2005 Area (Landsat TM)[1]
Southwall Hanging Glacier[4]	**0.029**	**0.022**	**0.015**	**0.028**	**0.025**	**0.005**
Main Area	0.029	0.022	0.015	0.028	0.025	0.000
Ice Mass 1						0.003
Ice Mass 2						0.002

Spatial resolution of data sources is 4, 15, and 30 m for the IKONOS, ASTER, and Landsat images, respectively. [1] Data obtained from Klein and Kincaid (2006). [2] The top number represents the total surface area of ice on Mt. Jaya (i.e. main glacier areas and small ice masses that have separated from the main glaciers) excluding the Southwall Hanging glacier (see text). The bottom number represents the total area for all glaciers measuring at least >0.1 km^2 (excluding the Southwall Hanging glacier: see Southwall Hanging glacier in results section). [3] These values represent the mapping results of the Carstensz glacier in the ASTER image plus the portion of the Carstensz missing from the ASTER scene. The area measurements for the missing portion were obtained by mapping the 2003 Landsat ETM+ image, which was acquired on the same day as the ASTER image. [4]Difficulties existed in mapping the Southwall Hanging glacier (see text) and the areas are not considered accurate. Therefore, these totals are only shown to indicate the magnitude in size of this glacier and are not included in the Mt. Jaya totals provided at the top of the table. *The resolution of the ASTER or Landsat images does not permit detection of these small ice masses.

glaciers larger than 0.1 km^2. These totals were 2.250, 2.101, 1.888, 2.069, 1.908, and 1.715 km^2 for the same dates, respectively.

Whereas, the Southwall Hanging glacier was observed in all of the images, the small size of this glacier, the rock overhang above it, and complex shadowing on the south facing glacier hindered accurate delineation of the glacier's boundaries. Based on the observations made from the IKONOS image it was determined that the Southwall Hanging glacier could not be measured accurately utilizing images acquired at the acquisition angles of the IKONOS, ASTER, and Landsat sensors. Therefore, it is not included in area totals.

6.2. Results from Comparing the 1972 and 1987 Glacier Areas to the 2000 to 2005 Areas

An error was discovered in the reporting of the Mt. Jaya glacier area for 1987 (Klein and Kincaid, 2006). Using the methods outlined in Section 5.5 of this thesis, the surface areas for the individual glacier systems in 1987 were 2.3, 1.3, 1.4, and <0.1 km^2 for the E. Northwall Firn/Meren glacier system, W. Northwall Firn, Carstensz glacier system, and the Southwall Hanging glacier, respectively, and the total surface ice area for Mt. Jaya was approximately 5.0 km^2. Peterson and Peterson (1994) reported that the total ice area on Mt. Jaya in 1987 was approximately 3.0 km^2.

Several lines of evidence suggest that the area of 5.0 km^2 is correct. The glacier extents represented on the 1987 map were measured using the scale bar provided within the map and the total of those areas closely approximate the 5.0 km^2 measurement. The 1987 map also illustrated the 1972 glacier extents. The surface ice area of the W.

Northwall Firn area as measured in a GIS from the 1987 map corresponded with those published in 1972. The W. Northwall Firn was selected for this process because it was the only glacier within the map for which the entire boundary was visible. As a last measure, the area of a small lake was measured from the 1987 map and found comparable in area to the measurement obtained from the 2002 IKONOS image. Therefore, the correct total for surface ice area on Mt. Jaya in 1987 was 5.0 km^2 and the surface areas for the individual glacier systems were 2.3, 1.3, 1.4, and <0.1 km^2 for the E. Northwall Firn/Meren glacier system, W. Northwall Firn, Carstensz glacier system, and the Southwall Hanging glacier, respectively. Glacier recession over the period from 1972 to 2005 is illustrated in Figure 18.

6.3. Climate Analysis Results

6.3.1. Frequency and Magnitude of El Niño

The climate analysis indicates that El Niño occurrences became more frequent and were of greater magnitude during periods 2 and 3 than those occurring in period 1. From the first to the second and second to third periods, the frequency of El Niño months increased by approximately 7.8% and 2.3%, while La Niña months decreased by 5.6% and 3.7%, respectively (Fig. 19). During the same time periods, neutral months decreased 2.2% and, then, increased by 1.4%. Specific to each time period, El Niño months accounted for 19.84%, 27.60%, and 29.91%, La Niña months accounted for

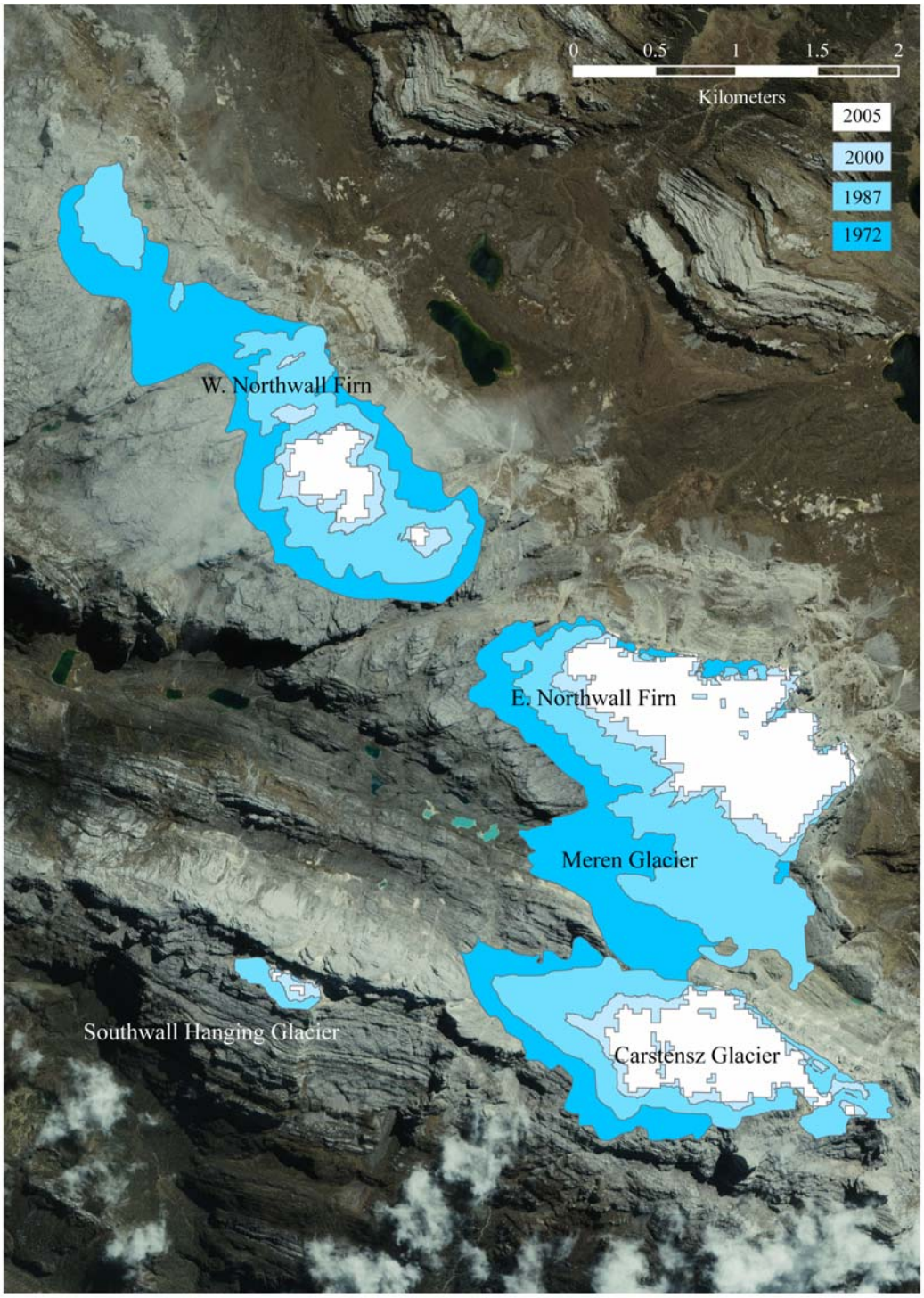

Fig. 18. Glacier recession on Mt. Jaya, Indonesia in 1972, 1987, 2000, and 2005. Glacier extents were determined in the field in 1972 (Hope and others, 1976), from a 1987 SPOT satellite image (Allison and Peterson, 1989), a 2000 IKONOS image (Klein and Kincaid, 2006), and a 2005 Landsat TM image.

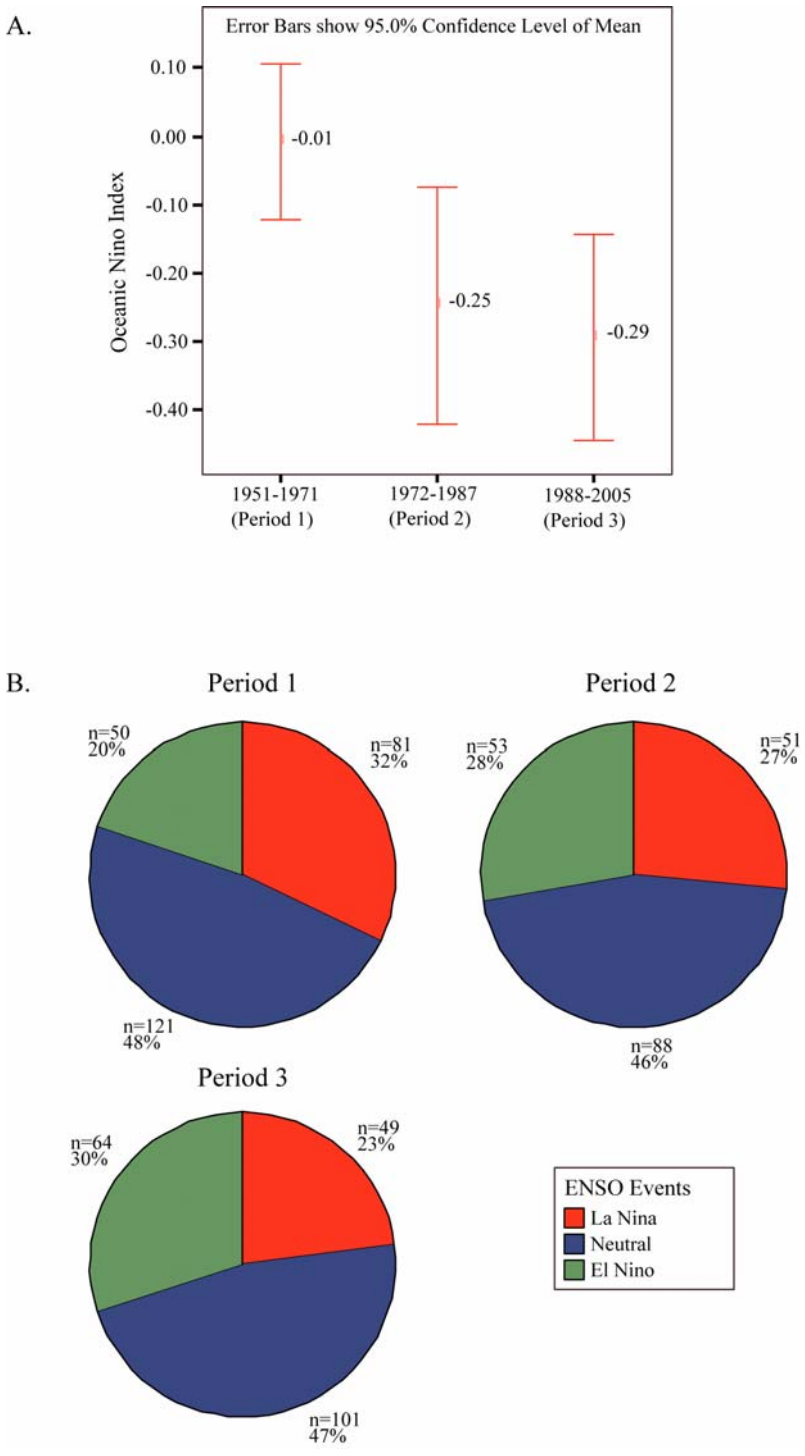

Fig. 19. Oceanic Niño Index and ENSO events. Graph A illustrates the mean monthly anomalies for the Oceanic Niño Index for each time period. B. Pie charts illustrate the frequency with which each ENSO phase occurred during each period.

32.14%, 26.56%, 22.90%, and neutral months accounted for 48.02%, 45.83%, and 47.20% of the total monthly events, respectively.

A statistically significant change (significance of t-test is 0.02 at 95% confidence level) in the overall mean for monthly ENSO anomalies is indicated between periods 1 and 2, but not for periods 2 and 3. From time period 1 to time period 2, the monthly anomalies decreased from -0.01 to -0.25. The monthly mean anomaly for period 3 was -0.29.

Analyzing the monthly changes in anomalies separately for each event category (i.e., El Niño, La Niña, and neutral events) indicates that a change in the magnitude of El Niño events is the reason for the shift towards more negative anomalies during the last two periods (Fig. 20). El Niño anomalies averaged -0.87 in period 1, whereas anomalies averaged -1.33 in period 2 (statistically significant at 0.01 for 95% confidence level). The mean anomalies during periods 2 and 3 were not statistically different, nor were anomalies for La Niña and neutral events over any of the periods tested.

6.3.2. Analysis of the Meteorological Variables

From period 1 to period 2, the mean monthly atmospheric temperature at 600 hPa increased by about 0.24°C, from 2.47°C to 2.71°C, and the freezing level rose by approximately 48 m, from 4854 m to an altitude of 4902 m. Cloud cover decreased by almost 4%, from 67 to 63%, precipitation at the surface decreased by about 7%, from 236 mm to 218 mm, radiation at the surface increased by 3%, from 232 watts m^{-2} to 238.5 watts m^{-2}, and wind speeds at 600 hPa decreased by about 7.5%, from 6.8 m s^{-1} to

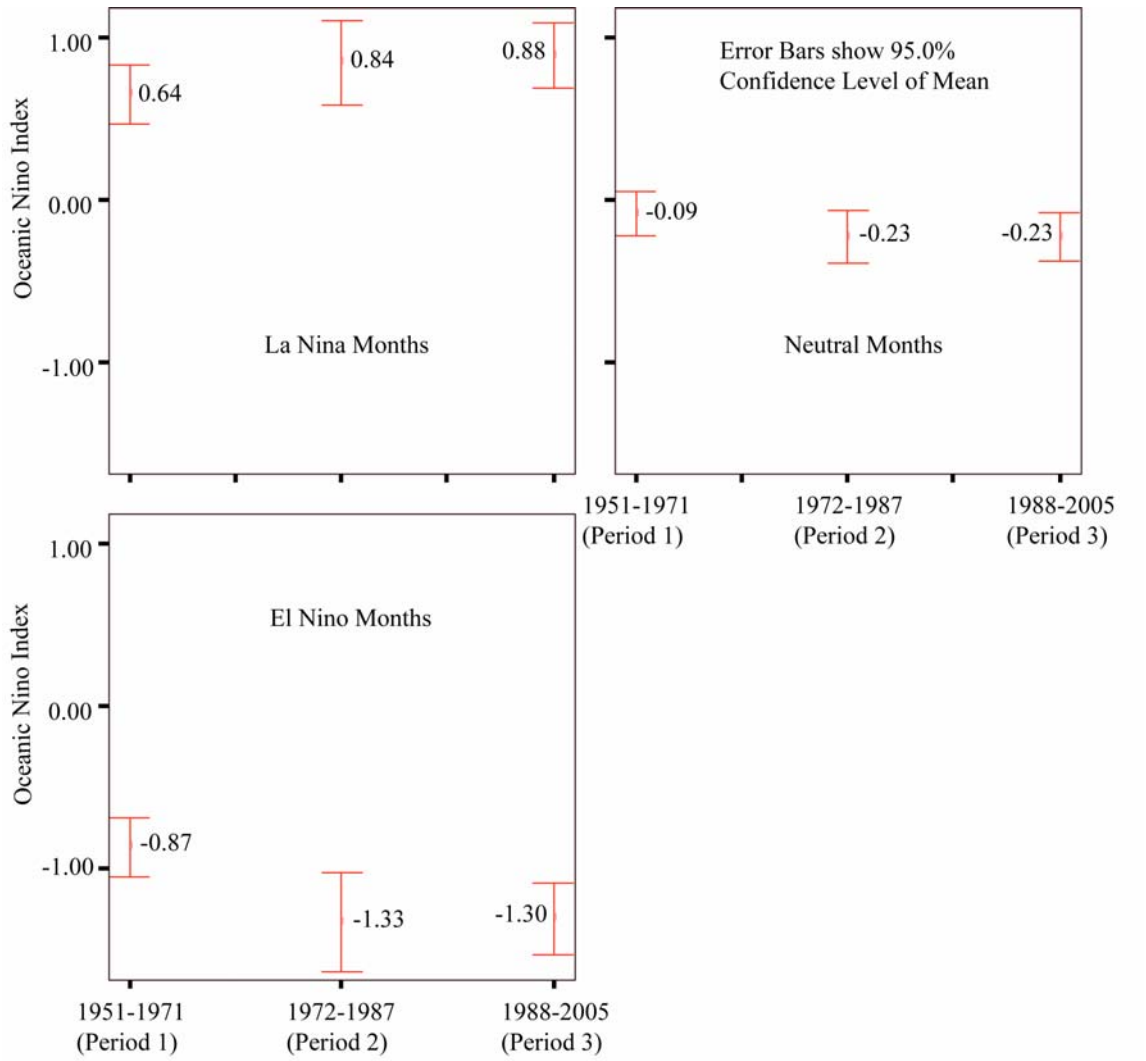

Fig. 20. Mean monthly Oceanic Niño Index anomalies during each period for La Niña, neutral, and El Niño months, respectively, from 1951 to 2005.

6.3 m s^{-1}. T-tests for statistically different means resulted in significance values of 0.000, 0.000, 0.000, 0.001, 0.000, 0.000 for the climate variables, respectively, at the 95% confidence level. The mean values for specific humidity at 600 hPa did not statistically change from period 1 to period 2 (Fig. 21, Table 3).

From period 2 to period 3, El Niño events became even more frequent, but the magnitude of the events remained approximately the same. However, mean monthly radiation decreased by approximately 1.7%, from 238.5 to 234.5 watts m^{-2}, precipitation at the surface increased by about 8%, from 218 mm to 235.8 mm, wind speeds at 600 hPa increased by 6.4% to 6.7 m s^{-1}, and specific humidity at 600 hPa increased by approximately 4%, from 4.05 to 4.2 g kg^{-1} (statistically significant at 0.027, 0.002, 0.002, 0.006, respectively, at the 95% confidence level). Atmospheric temperature, the freezing level, and percent cloud cover did not statistically change from their 1972-1987 mean.

6.3.3. Climate Variables and ENSO

Monthly means of atmospheric temperature, freezing level, and percent cloud cover during periods 1, 2, and 3 all change similarly to the change in the magnitude of ENSO anomalies, with statistical differences in the mean values only between periods 1 and 2. Whereas atmospheric temperature and freezing level rise with El Niño, percent cloud cover decreases. Monthly means for precipitation, wind speeds, and radiation all have significant differences between periods 1 and 2 and periods 2 and 3. While following the same trend as the ENSO anomalies, the magnitude of change in monthly mean values for specific humidity in the Mt. Jaya area does not indicate a relationship.

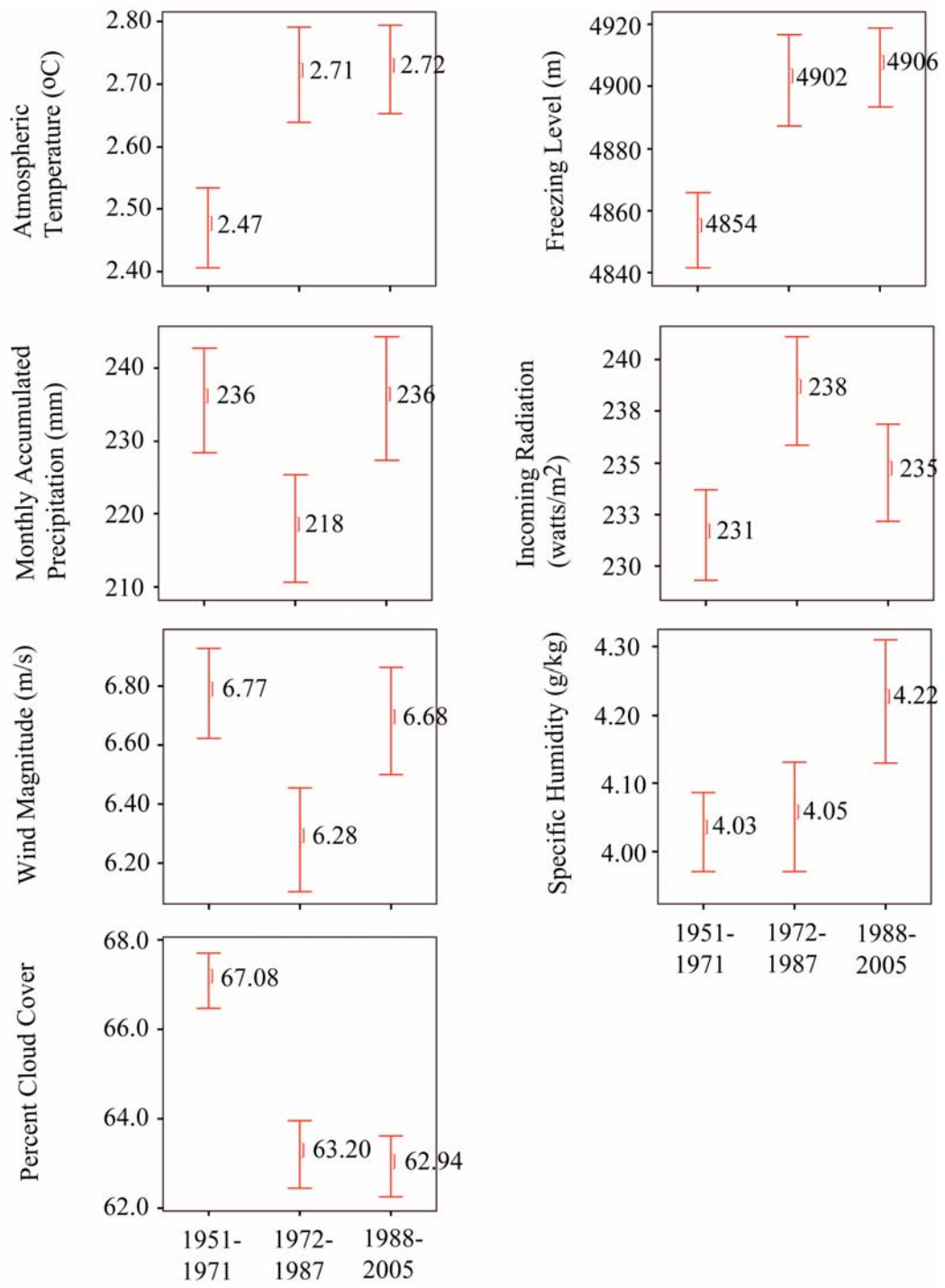

Fig. 21. Monthly means for temperature, freezing level, precipitation, incoming radiation, wind magnitude, specific humidity, and percent cloud cover during each time period.

Table 3. Climate changes from 1951-2005. The magnitude of change over each time period for each climate variable and the significance of the t-test are shown. Values in bold indicate that the mean during that period significantly changed.

	Magnitude of Change From Period 1-2	**T-test**	**Magnitude of Change From Period 2-3**	**T-test**
ONI Anomalies	**-0.24**	0.024	**-0.04**	0.682
Atmospheric Temperature	**0.24°C**	0.000	0.01°C	0.881
Freezing Level	**48.3 m**	0.000	4.12 m	0.673
Precipitation	**-17.55 mm**	0.001	**17.86 mm**	0.002
Radiation	**7.0 watts m^{-2}**	0.000	**-3.96 watts m^{-2}**	0.027
% Cloud Cover	**-3.87%**	0.000	-0.26%	0.615
Specific Humidity	0.02 g kg^{-1}	0.655	**0.17 g kg^{-1}**	0.006
Wind Speeds	**-0.5 m s^{-2}**	0.000	**0.13 m s^{-2}**	0.002

7. DISCUSSION

7.1. Comparisons of the Mapping Results Obtained Using ASTER and Landsat ETM+ Images

Acquisition of images of the Mt. Jaya glaciers on May 29, 2003 by both Landsat and ASTER provides a unique opportunity to compare glacier areas of these small glaciers from two sensors. In Table 2, it can be seen that the surface ice areas mapped from the Landsat image consistently resulted in larger surface areas for the glaciers. More specifically, the main areas of the glaciers were 5.3%, 11.2%, and 18.9% larger for the E. Northwall Firn, Carstensz, and W. Northwall Firn, respectively, when mapped from the Landsat image. There is also a pattern of increasing difference in the mapping between the two sensors with decreasing glacier area.

7.2. Overall Changes in Glacier Extents on Mt. Jaya from ca. 1850 to 2005

7.2.1. Description of Tables and Figures Compiling Observations from ca. 1850-2005

Tables 4 through 6 present the compilations of the glacier surface areas recorded for Mt. Jaya over the past century as published by Allison (1974), Allison and Peterson (1976), Allison and Peterson (1989), Klein and Kincaid (2006) and the results of this work for 2003-2005. Table 4 provides the areas of the major systems, whereas Tables 5 and 6 discriminates between the individual glaciers comprising the Northwall Firn/Meren and Carstensz glacier systems, respectively. The Northwall Firn/Meren glacier system consists of the E. and W. Northwall Firns, and the Meren and Harrer glaciers, while the Carstensz, Wollaston, and Van de Water glaciers comprise the Carstensz glacier system.

Table 4. Ice surface areas (km^2) for the Mt. Jaya glaciers from ca. 1850 to 2005.

	Entire Mt. Jaya Area	Northwall Firn and Meren Glacier	Total Carstensz System	Southwall Hanging Glacier	Harrer Glacier
Neoglacial (ca 1850)[1]	19.3	*14.2*	3.6	1.0	0.5
1913[1]				0.4	
1936[1]	13	11.1	1.6	0.3	<0.1
1942[1]	9.9	8.1	1.5	0.3	<0.1
1962[1]					<0.1
1972[1]	6.9	5.5	1.2	0.2	<0.1
1972[2] (corrected)	7.3	*5.8*	1.4	0.1	
1974[2]	*6.4* *[6.6]*	*4.9*	1.4	0.1	
1987[3]	3.0 [5.0][5]	[3.6][5]	[1.4][5]	[<0.1][5]	
2000[4]	2.25	1.52	0.73	<0.1	
2002[4]	2.10	1.42	0.69	<0.1	
2003	1.89	1.26	[0.63][6]	<0.1	
2003	2.07	1.36	0.71	<0.1	
2004	1.91	1.30	0.61	<0.1	
2005	1.72	1.17	0.55	<0.1	

Italicized values represent our totals computed from published areas. [1]Allison (1974) and Allison and Peterson (1976). [2]Allison and Peterson (1989). [3]Peterson and Peterson (1994). [4]Klein and Kincaid (2006). To facilitate comparisons, only the areas of ice masses >0.1 km^2 are given. [5]These values were computed from the mapped glacier areas on the Peterson and Peterson (1994) map (see text). [6]This value was computed by adding the tail of the Carstensz, as measured on the 2003 Landsat ETM+ image, on to the area measured from the 2003 ASTER image (see text).

Table 5. Ice surface areas (km^2) for individual glaciers comprising the Northwall Firn/Meren glacier system from ca. 1850 to 2005.

	Northwall Firn and Meren Glacier	W. and E. Northwall Firn[6]	W. Northwall Firn[6]	W. Northwall Firn (A)	W. Northwall Firn (B)	E. Northwall Firn[6 & 7]	Meren Glacier[7]	E. Northwall Firn and Meren Glacier[7]
Neoglacial (ca 1850)[1]	***14.2***	9.1					5.1	
1913[1]								
1936[1]	**11.1**	8.3	6.7			1.6	2.8	4.4
1942[1]	**8.1**	5.5	4.4			1.1	2.6	3.7
1962[1]							2.1	
1972[1]	**5.5**	3.6	2.5			1.1	1.9	3.0
1972[2] (corrected)	***5.8***	3.6					2.2	
1974[2]	***4.9***	2.8					2.1	
1987[3]	**[3.6][5]**			[1.12][5]	[0.18][5]			[2.3]
2000[4]	**1.52**			0.29	0.00			1.23
2002[4]	**1.42**			0.25				1.17
2003	**1.26**			0.20				1.06
2003	**1.36**			0.24				1.12
2004	**1.30**			0.21				1.08
2005	**1.17**			0.18				0.98

Only ice masses >0.1 km^2 are given. [1]Allison (1974) and Allison and Peterson (1976). [2]Allison and Peterson (1989). [3]Peterson and Peterson (1994). [4]Klein and Kincaid (2006). [5]These values were computed from the mapped glacier areas on the Peterson and Peterson (1994) map (see text). [6]The W. and E. Northwall Firn areas were observed as one contiguous ice mass in 1936 and 1942. The ice masses separated sometime between 1942 and 1962 (Allison and Peterson, 1976). [7]The boundary between the E. Northwall Firn and Meren glacier shifts (see text). Sometime between 1987 and 1992 the tongue of the Meren separated from the rest of the glacier and completely melted by 2000.

Table 6. Ice surface areas (km^2) for the individual glaciers comprising the Carstensz glacier system from ca. 1850 to 2005.

	Total Carstensz System	Carstensz Glacier	Wollaston Glacier	Van de Water Glacier
Neoglacial (ca 1850)[1]	**3.6**	2.5	0.5	0.6
1913[1]			0.3	0.2
1936[1]	**1.6**	1.25	0.2	0.15
1942[1]	**1.5**	1.1		
1962[1]		0.95		
1972[1]	**1.2**	0.89	0.17	0.14
1972[2] (corrected)	**1.4**	*	*	*
1974[2]	**1.4**	*	*	*
1987[3]	**[1.4][5]**	*	*	*
2000[4]	**0.73**	*		*
2002[4]	**0.69**	*		*
2003	**[0.63][6]**	*		*
2003	**0.71**	*		*
2004	**0.61**	*		*
2005	**0.55**	*		*

[1]Allison (1974) and Allison and Peterson (1976). [2]Allison and Peterson (1989). [3]Peterson and Peterson (1994). [4]Klein and Kincaid (2006). To facilitate comparisons, only the areas of ice masses >0.1 km^2 are given. [5]These values were computed from the mapped glacier areas on the Peterson and Peterson (1994) map (see text). [6]This value was computed by adding the tail of the Carstensz, as measured on the 2003 Landsat ETM+ image, on to the area measured from the 2003 ASTER image. *Distribution unknown.

Providing information on both the individual glaciers and the glacier systems was necessary to adequately compare the glacier areas and to calculate the rates of loss over a century long record of recession. Over the past century not only has the Northwall Firn divided into the E. and W. Northwall Firns, but also, the Harrer, Meren, and Wollaston glaciers, the latter two flowing from other ice masses on the mountain, have melted. As these glaciers receded, ice flow patterns in the firn areas shifted resulting in redistributing the area between the glaciers sharing the firn field. For example, the 1972 measurements of the area distribution of the E. Northwall Firn and Meren glaciers were made based on identifying flow lines and the portions of the E. Northwall Firn that were contributing to the Meren glacier. (Allison, 1974; Allison and Peterson, 1989). It was expected that the dividing line between the E. Northwall Firn and Meren glacier would continue to shift as the Meren glacier receded. Although the Meren glacier is now gone and it appears from the mapping that the E. Northwall Firn is all that remains, reporting an area measurement for the E. Northwall Firn of 1.23 km^2 for 2000 would suggest that the firn field has grown when it has actually greatly receded from its 1972 surface area. Using the 1-meter IKONOS images it is not possible to identify flow-lines, and thereby, discriminate what may remain of the Meren glacier. Therefore, the E. Northwall Firn and Meren glacier will be called the E. Northwall Firn/Meren glacier system after 1974, when the last measurements were made for the Meren glacier.

Both the original 1972 and the corrected 1972 values are shown in the Tables 4-6. However, only the corrected values were used in calculating rates of ice loss (Table 7).

Table 7. Rates of ice loss (km^2/year) for the Mt. Jaya glaciers from ca. 1850 to 2005.

Glacier	**ca 1850 to 1913**	**1913 to 1936**	**1936 to 1942**	**1942 to 1962**	**1962 to 1972**	**1972 to 1974**	**1974 to 1987**	**1987 to 2000**	**2000 to 2002**	**2002 to 2003[2]**	**2003[2] to 2004**	**2004 to 2005**
Mt. Jaya	**0.07**		**0.52**	**0.09**		**0.45**	**[0.11][1]**	**[0.21][1]**	**0.07**	**0.21**	-0.02	**0.19**
			0.16			**0.15**				0.03	**0.16**	
Northwall Firn and Meren Glacier	**0.04**		**0.5**	**0.08**		**0.45**	**0.10**	**0.16**	**0.05**	**0.16**	-0.04	**0.13**
			0.15			**0.15**				0.05	**0.06**	
W. and E. Northwall Firn	0.01		0.47	0.06		0.40						
			0.13									
W. Northwall Firn			0.38	0.06		[0.08][1]		[0.08][1]	0.02	*0.05*	-0.01	0.03
			0.12							0.01	*0.03*	
Meren Glacier	0.03		0.03	0.03	-0.01	0.05						
			0.02									
E. Northwall Firn and Meren			0.12	0.02		0.05		0.08	0.03	*0.11*	-0.02	0.10
			0.04							0.05	*0.04*	
Total Carstensz System	**0.02**		**0.02**	**0.003**		**0**	**0**	**0.05**	**0.02**	**0.06**	0.02	**0.06**
			0.01			**0**				-0.02	**0.10**	
Southwall Hanging Glacier	**0.01**	**0.004**	**0.0**	**0.01**		**0**						
	0.01		**0.01**									

[1]This value was computed using the combined values for both the W. Northwall Firn A and B in 1987. [2] In the 2002-2003 and 2003-2004 columns the top and bottom values for each glacier represent the rates of recession calculated with the results obtained from mapping the 2003 ASTER and 2003 Landsat ETM+, respectively.

The recession of the Mt. Jaya glaciers from ca. 1850 to 2005 is graphically illustrated in Figure 22.

Whereas the Mt. Jaya glaciers are well-studied and have a long record of observations, the chronology presented here is coarse. This is a common problem for most all glacier records, and especially those of the tropics (Kaser, 1999). In making comparisons between the rates of recession, most all of which have occurred over time intervals of varying length, it is important to note that there is not an implication that high or low rates of recession existed over an entire period or that periods of high or low rates did not occur at other times during the century. They simply represent periods in which it is known that at some point during that time period exceptionally high rates of recession occurred. An examination of the 2000-2005 rates of ice loss in Table 7 illustrates the degree of fluctuation that can occur between annual time periods.

7.3. Detailed Changes for the Northwall Firn and Meren Glacier System

Overall, the Northwall Firn and Meren glacier system dominates the recessional trend for the total Mt. Jaya area. From ca. 1850 to 2005 the system lost 13.0 km^2 of its surface ice area representing 91.5% of its ca. 1850 area. In 1936, Dozy (1938) described the Northwall Firn system as one contiguous firn field. This glacier system split into two parts at the New Zealand Pass sometime between 1942 and 1962 (Allison and Peterson, 1976), resulting in the W. Northwall Firn and the E. Northwall Firn/Meren glacier systems.

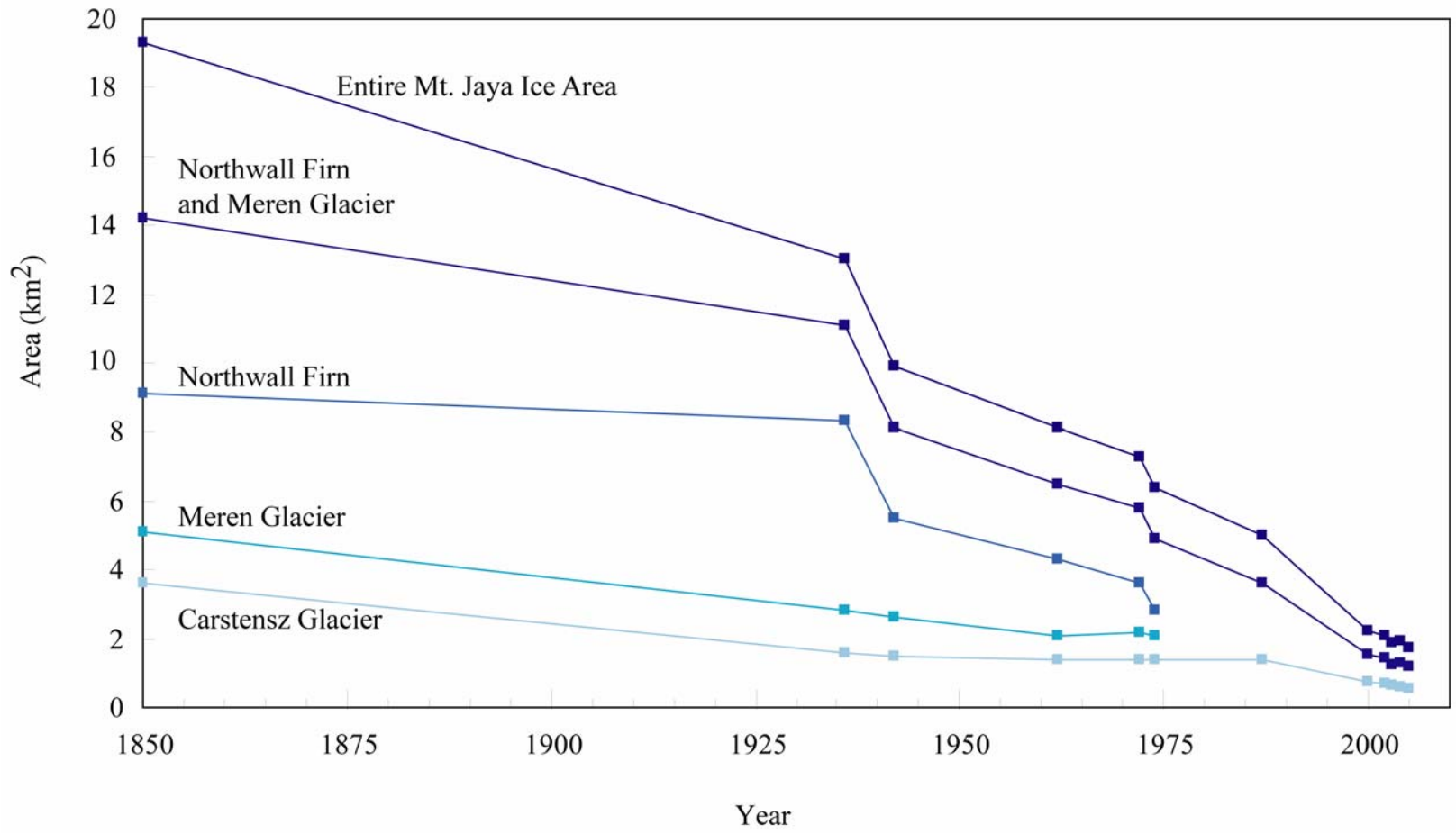

Fig. 22. Surface ice areas for the Mt. Jaya glaciers from ca. 1850 to 2005. Squares represent data points for observations over the time period.

7.3.1. E. Northwall Firn/Meren Glacier System

Total area measurements, obtained from fieldwork for the E. Northwall Firn/Meren glacier system were provided as early as 1936. This system decreased in area by 3.4 km^2, from 4.4 km^2 in 1936 to 0.98 km^2 in 2005. This loss represents 24% of the surface area of the entire Northwall Firn/Meren system and 18% of all surface ice existing on Mt. Jaya at the LIA maximum.

Between ca. 1850 and 1974 the Meren glacier lost 3.0 km^2 of its surface ice area, constituting almost 59% of its ca. 1850 area. The Meren glacier formerly flowed into the Meren Valley from the most eastern portion of the E. Northwall Firn. Using data from the 1972 field expeditions, Allison and Kruss (1977) numerically modeled the Meren glacier and predicted that increased melting would likely occur over the next several years. In 1992, during a field expedition, Peterson and Peterson (1994) observed that the tongue of the Meren glacier had separated from the E. Northwall Firn and predicted that within a few short years it would no longer exist. Observations made from the 2000 IKONOS image indicate that the tongue of the Meren glacier has completely melted.

As illustrated in Figure 18, the E. Northwall Firn/Meren system has primarily receded along its southwest and western borders. However, some recession has occurred along most all borders from 1987 to 2005. Hypsometries, for 1972, 1987, and 2002 determined from SRTM topography (Klein and Kincaid, 2006), illustrating the recession in regards to elevation are shown in Figure 23. The hypsometry indicates that the E. Northwall Firn/Meren glacier is losing surface area at all elevations, with the majority of

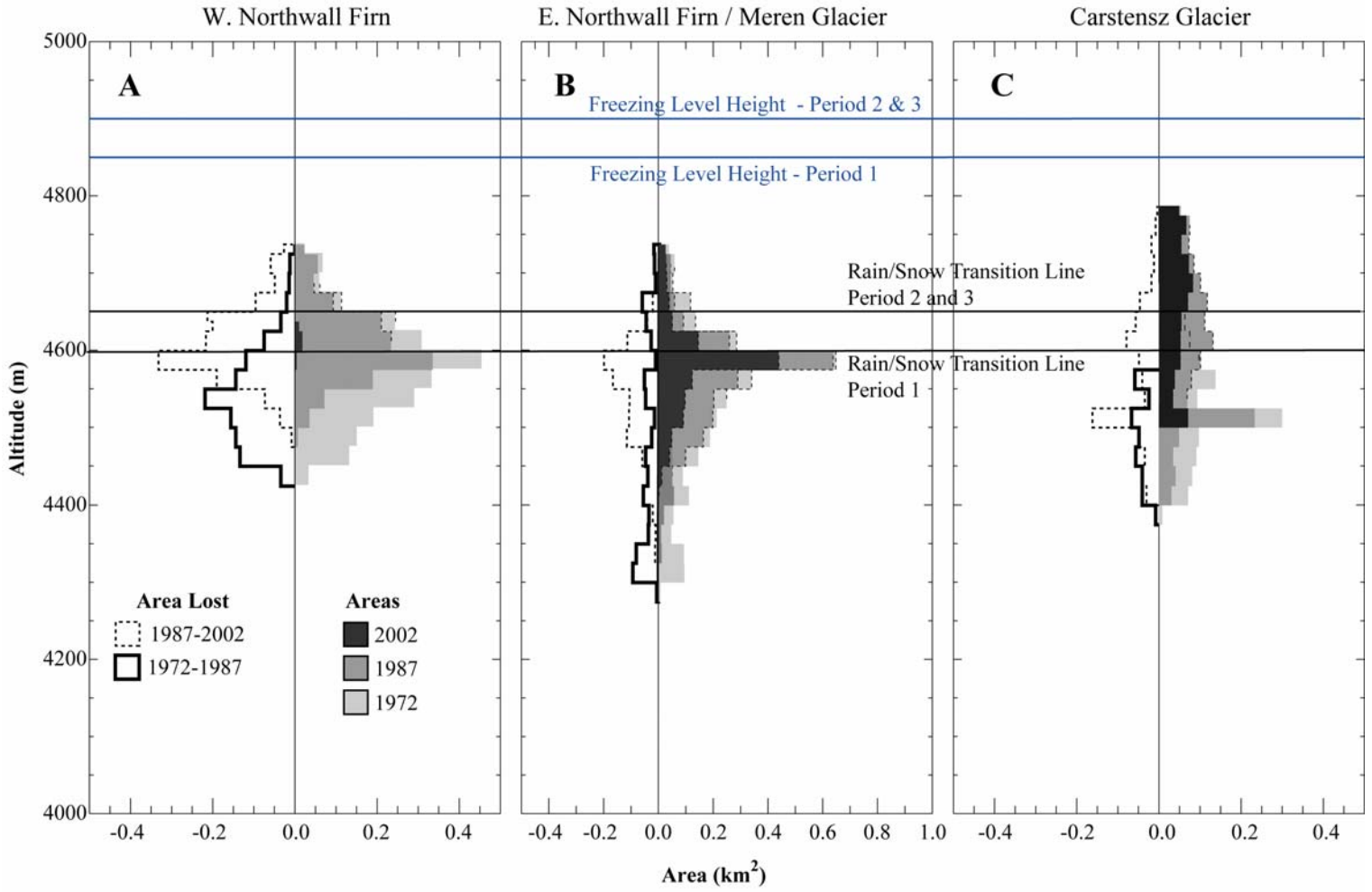

Fig. 23. Hypsometries for the W. Northwall Firn, the E. Northwall Firn/Meren glacier system, and the Carstensz glacier for 1972, 1987, and 2002. Map modified from Klein and Kincaid (2006).

ice loss having shifted to higher elevations between the intervening periods. This pattern of loss suggests that the elevation range for this firn field is shrinking.

Evidence of ice thinning is also apparent in as the number of rock protrusions increased between 2000 and 2005. Whereas the SRTM data used to produce the topographic map for this thesis is too coarse for providing detailed topography over the glacier, the 1972 survey map indicates that these rock protrusions are in an area surrounding a peak in elevation of 4810 m.

7.3.2. W. Northwall Firn

From 1936 to 2005, the W. Northwall Firn lost approximately 6.52 km^2 of its surface ice area, representing 97% of its 1936 area. This loss also represents 59%, and 50% of the surface ice area of the Northwall Firn/Meren system and the Mt. Jaya ice areas measured for 1936, respectively. A period of extreme ice loss occurred between 1936 and 1942 resulting in a loss of approximately 34% of its surface area over this short period. While the acquisition of surface area measurements was not frequent enough to constrain the loss to these years, this time period of excessive retreat is consistent with the behavior of other tropical glaciers, worldwide (Kaser, 1999).

The W. Northwall Firn began disintegrating sometime after 1972. Allison and Peterson (1989) reported that this glacier was observed as three separate ice masses in a 1983 Landsat image. One of these ice masses, which no longer exists, lied outside the area shown in the 2000-2005 mapping as illustrated in Figure 18. In 1987, two ice masses were observed and by 2000 only one ice mass was observed with an area >0.1 km^2. Spatially, over the past century this firn field has predominantly receded from the

west. Whereas this firn field is primarily receding from its lowest elevations, ice loss substantially increased at higher elevations between 1987 and 2000, at which time recession slowed substantially.

7.4. Detailed Changes for the Carstensz Glacier System

Overall, the Carstensz glacier system receded from a surface area of 3.6 km^2 in ca. 1850 to an area of 0.55 km^2 in 2005, representing a loss of 98.5% of its original area and representing 19% of the entire Mt. Jaya ice area. Similar to the Meren glacier, rates of recession calculated for the Carstensz glacier from 1936-1942 were not nearly as high as for the Northwall Firn areas. Along the north and eastern ridges of the Carstensz glacier small portions of the 2002 mapping extended past the maximum areas delineated from the 2000 image. It is unlikely based on the overall trend in the area that the glacier has grown and these areas are most likely a result of coregistration errors or possibly snow-cover rocks. Overall, these areas account for only approximately 0.2% of the 2000 glacier area.

From field observations in 1992, Peterson and Peterson (1994) reported that the Wollaston glacier was nearly gone. Although it is difficult to distinguish between the boundaries of the Wollaston glacier and the Carstensz glacier in the satellite images, the magnitude of melt along the southern edge of the border from 1987 to 2000 suggests that the Wollaston glacier has melted. The same situation applies for the Van de Water glacier in that its boundaries are indistinguishable from the Carstensz glacier. Comparisons of earlier maps with the results obtained in the 2000-2005 mapping indicates that it has either melted or that the tail of the Carstensz is all that remains.

For 1987-2005, recession occurred along the entire circumference of the Carstensz glacier system (Figures 18 and 23). However, this was not the case from 1972-1987 during which ice loss was primarily restricted to the lower elevations of the glacier. The greatest recession has occurred along the tongue of the Carstensz glacier, along the entire southern border of the Carstensz system, and along the tail of the Carstensz system. Six small ice masses were observed in the 2000 image along the eastern edge of the glacier indicating rapid disintegration in the tail area. Only two of these ice masses remained in 2002 and only one was observed in the 2003-2005 images. From 2003-2005, most of these very small ice masses probably melted, but others may not have been detectable as a result of the lower spatial resolution of the ASTER and Landsat images. In addition to these observations, a large portion of the tongue of the Carstensz glacier appears to be severely thinning as indicated by the increase in number and the pattern of rock protrusions observed from 2000-2005.

7.5. The Rates of Recession for the Mt. Jaya Glaciers are Accelerating

Sporadic observations over the past century have highlighted some periods of exceptionally high rates of ice loss for the area, such as from 1936-1942, 1972-1974, and 1987-2000. In general, the 1936-1942 and 1987-2000 periods correspond well with periods of higher recessional rates for tropical glaciers and for other glaciers world-wide (Kaser, 1999). However, the 1972-1974 period does not correlate well. Kaser (1999) reports that the 1970s was a period of stable conditions, with some tropical glaciers slightly advancing. The high ice losses for the Mt. Jaya area from 1972-1974 solely represents the area losses from the Northwall Firn/Meren glacier system. No area losses

were reported for the Carstensz glacier from 1972-1987 and the state of this glacier during the 1970s does correspond with other tropical glaciers. The lower area losses for the Carstensz glacier when compared to the Meren glacier can be attributed to the higher elevation of its firn field and the steeper valley in which it flows (Peterson and Peterson, 1994; Allison, 1974). Overall, Kaser (1999) notes that the Irian Jaya glaciers are receding at much quicker paces than most other tropical glaciers similar in size and attributes this to the smaller elevation range on which they are located.

From ca. 1850 to 2005, the Mt. Jaya glaciers retreated from 19.3 km^2 in area to 1.72 km^2, amounting to a 91% surface ice area loss since the LIA maximum. As is illustrated in Figure 22, from ca. 1850 to 1936, the Carstensz and Meren glaciers dominated the recessional trend for the area. This trend was reversed from 1936-2003 with the Northwall Firn/Meren system dominating the area losses. Closer examination of the Northwall Firn/Meren system (Fig. 24) indicates that from 1936-2000 the high surface area losses for the W. Northwall Firn overshadowed those of the E. Northwall Firn, which appears to have maintained a constant surface ice area from 1942-1972. Higher rates of loss for the E. Northwall Firn/Meren system from 1972 to sometime between 1992 and 2000, when the Meren glacier completely melted, were primarily controlled by the rapid recession of the Meren glacier. After 2000, the E. Northwall Firn continued to lose ice at higher rates. The Carstensz glacier maintained low recessional rates from1942 to 1987, but these rates began to increase around 1987 and have remained high into 2005.

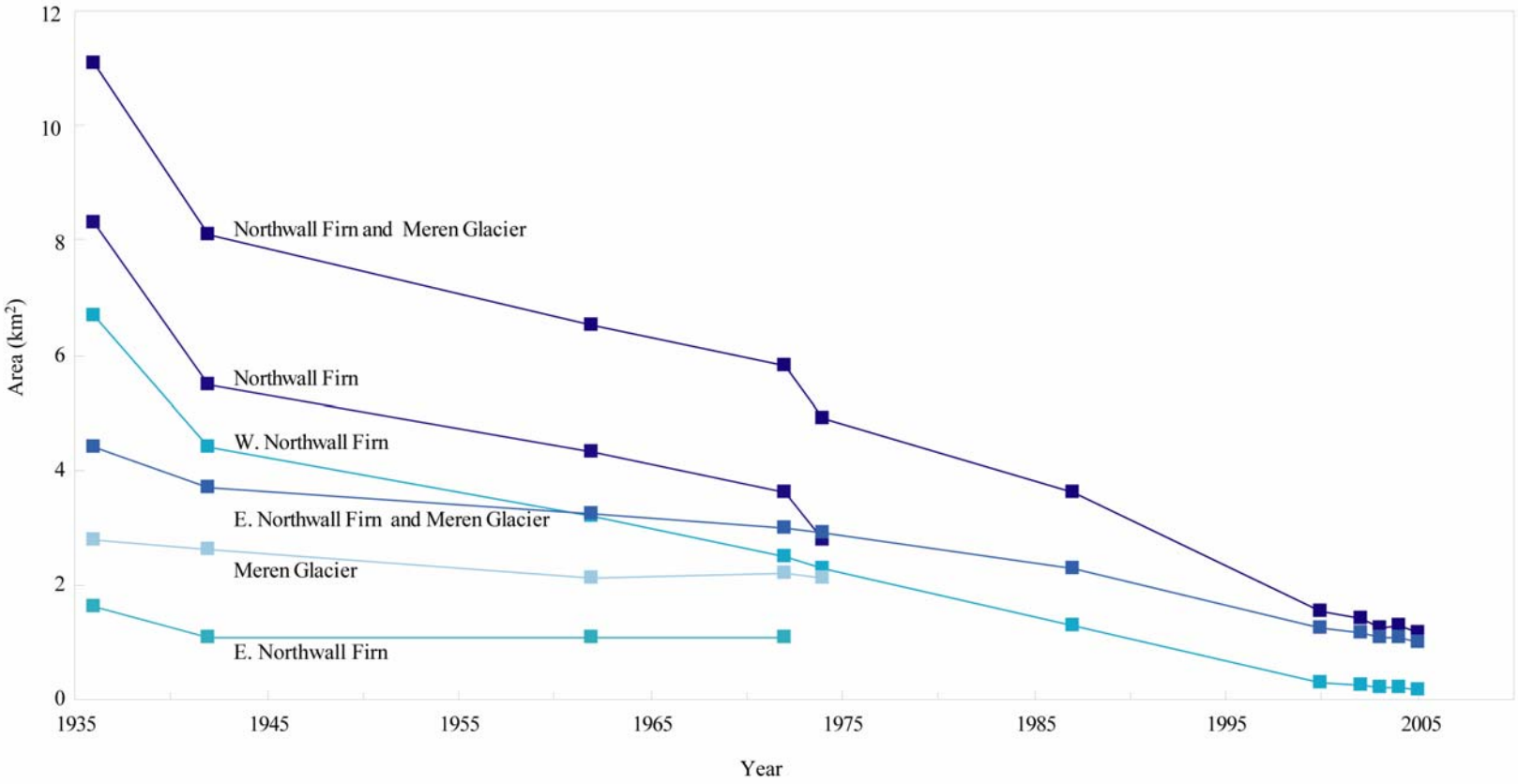

Fig. 24. Surface ice areas for the Northwall Firn and Meren glacier from 1936 to 2005. Squares represent data points from observations made during this time period.

7.6. Relationship of Climate Variables to Glacial Recession

According to the studies on the inner tropical glacier, Antizana 15 (Favier and others, 2004b), El Niño years are accompanied by higher temperatures, less precipitation, lower specific humidity, and lower wind speeds. These conditions appear to affect the Mt. Jaya glaciers as well as El Niño events became more frequent and of greater magnitude in period 2. In addition, radiation increased and cloud cover decreased. Although ice loss from 1942-1972 was less than that for period 2, the amount that occurred between 1951 (the time period for which climate data is available) and 1972 is not known and therefore, some uncertainty does exist in the amount of ice loss for period 1. However, according to numeric modeling (Kaser and Osmaston, 2002) an increase in temperature of 0.24°C (the magnitude of change occurring between periods 1 and 2) would have resulted in an increase in the ELA of approximately 70 m. Changes in the other climate variables were not of a magnitude sufficient to have caused the increase in ice loss. This result suggests that rising temperatures and freezing level heights are the primary reason for increased ice loss between these two periods.

However, rising temperatures alone does not explain the acceleration of ice loss between periods 2 and 3. Between these two periods, the frequency of El Niño months increased, but the magnitude of the monthly events did not significantly change, nor did temperature. The only variables that did significantly change were specific humidity, wind, precipitation, and radiation, all increasing except the latter. A decrease in radiation, as well as increased precipitation would result in reducing ice loss, whereas increases in specific humidity and stronger winds would increase sensible heat inputs to

the glaciers and result in increased melt. It is unlikely that the increase in specific humidity was of sufficient magnitude to account for the increased ice loss or to offset the reduction in radiation and the increase in precipitation.

On Antizana 15 glacier, increased quantities of precipitation were occurring in rain phase as opposed to snow as a result of higher temperatures and freezing levels. Precipitation/rain phase may be having a major impact on the Mt. Jaya glaciers as observed in the 2000 through 2005 satellite images. Prentice (2005) calculates that the snow/rain transition boundary is at approximately 250 m below the freezing level for the Mt. Jaya glaciers. Examination of the glaciers within the 2000-2005 satellite images suggests that this may be a good estimate as melt water ponds are visible in the images at around elevations obtained utilizing Prentice's estimation. Specifically, the snow/rain transition is estimated at 4606 m, 4706 m, 4701 m, 4680 m, and 4720 m for the 2000-2005 images, respectively, using the freezing levels computed from the NCEP/NCAR Reanalysis data. Calculations for the snow/rain transition for periods 1-3 result in a transition line at 4604 m for the former period and approximately 4654 m during the latter two. While the boundary line for the precipitation phase did not rise during the third period, the amount of precipitation did increase which would have resulted in increased ice loss, especially thinning.

8. CONCLUSIONS

With the exclusion of the 1936-1942 rates of ice loss, the overall ice loss for the Mt. Jaya glaciers does appear to have increasingly accelerated over the past century. The Meren glacier disappeared sometime between 1991 and 2000, as most likely did the Wollaston glacier. By 2005, the Van de Water glacier no longer was observable in the images.

However, closer examination of the individual glacier systems indicates that the ice loss for all of the glaciers was not increasingly accelerating over the entire century. The overall rates of ice loss on Mt. Jaya were dominated by the W. Northwall Firn throughout most of the century until 2000 when only one small ice mass remained that was at least >0.1 km^2. It is difficult to access the ice loss for the E. Northwall Firn after 1972 as the next recorded observation was not until 1987 and this area measurement included the Meren glacier which was increasingly deteriorating. The literature does indicate that from 1942-1972 the E. Northwall Firn was not experiencing the same degree of ice loss as the W. Northwall Firn and actually maintained a fairly consistent area of ice over that same period.

The mapping indicates that, sometime after 1972, ice loss for the E. Northwall Firn began to increase. The Meren glacier, the largest valley glacier in the area, lost ice at a fairly consistent rate over the first half of the century. It was not until sometime after 1972 that this glacier began to lose ice at increasingly accelerated rates. Finally, the ice loss rates for the Carstensz glacier indicate that ice loss was decreasing for this glacier over most of the past century with no ice loss at all from 1972-1987. Only sometime

after 1987 did this glacier begin to lose ice at increasing rates. Therefore, with the exception of the W. Northwall Firn, and for the E. Northwall Firn during the time period 1936-1942, area losses for the ice masses on Mt. Jaya did not accelerate until after 1972.

Overall, several periods of high recessional rates are observed in the Mt. Jaya glacier record: 1936-1942, 1972-1974, 1987-2000, and 2002-2005. The recession of the Mt. Jaya glaciers, during the periods from 1936-1942 and 1987-2000, correlate well with the recessional trend of glaciers world-wide during the same time periods (Kaser, 1999). However, the correlation in losses for 1936-1942 is primarily a result of the high amounts of ice loss occurring on the Northwall Firn. More studies would have to be completed to confirm that the Meren and Carstensz glaciers followed the same accelerated recessional trend as other glaciers during this period. According to Kaser (1999), the 1970s were a period of stability for most tropical glaciers, with some even advancing. While the Carstensz glacier did maintain a consistent area of ice throughout the 1970s, the other ice masses on Mt. Jaya experienced increased ice loss during this period when compared to earlier periods.

The overall trend for the ONI indicates that the frequency and magnitude of El Niño events increased in the 1970s and were consistently strong thereafter. At the same time, ice loss on Mt. Jaya accelerated suggesting that a relationship may exist between the increase in negative ONI anomalies (i.e., El Niño events) and the accelerated retreat of the glaciers. Additional studies are needed to determine if this relationship does exist.

Overall, El Niño events for Indonesia should result in higher temperatures, decreased precipitation, increased solar radiation, decreased cloud cover, and an increased

proportion of the overall precipitation occurring in rain phase, all of which would cause an increase in recession rates for the glaciers. Statistically, at the 600 hPa pressure height over the Mt. Jaya area, temperatures did increase by 0.24° C from the period 1951-1971 to the period 1972-1987 and remained consistently higher through 2005 than temperatures before this time period. As a result of higher temperatures, the freezing level height increased approximately 50 m over the same time period. According to Kaser's mass balance model, a 24°C increase in temperature would result in an ELA increase in elevation of approximately 70 m. Cloud cover also decreased as did precipitation, whereas incoming radiation increased. While this correlates well with the increased recession of the Mt. Jaya glaciers overall, the Carstensz glacier did not retreat during this time period. Additionally, while anomalies in the ONI remained consistently negative during the time period from 1987-2005, temperatures did not increase and some climate parameters, such as an increase in precipitation and a decrease in radiation, shifted to conditions favorable for glacial advances. However, the glacial retreat on Mt. Jaya continued to accelerate during this time period. Accelerated retreat could have been caused by several factors. First, if the increase in precipitation was accompanied by increases in rain as the primary phase, this would have resulted in increased melt. Second, perhaps an imbalance of a larger magnitude than that for which the glaciers could recover existed. Observations of melt ponds over most of the glacier surfaces, especially extensive in the 2005 image, suggests that the glaciers can no longer recover under the current climate conditions.

While it is not possible to conclusively assign causation of the recession to any of the climate variables, application of the results Kaser and Osmaston (2002) obtained in modeling ELA changes indicate that a temperature rise is the most likely explanation for the recession of the Mt. Jaya glaciers. The 0.24°C increase in temperature from period 1 to period 2 in the Mt. Jaya region would result in an approximate rise in the ELA by about 70 m. At the same time, the magnitudes of the changes in the other climate variables over the region were not sufficient to have had such an impact on the ELA. However, it is obvious that ice loss for the glaciers increased even more from 1987 to 2005 and this cannot be accounted for by the 0.1°C increase in atmospheric temperature that occurred during the same time period. All of this suggests that the explanation for increased recession is much more complicated than can be explained through a direct relationship to temperature and that additional studies are needed.

Indications that El Niño events are increasing in both frequency and magnitude as a result of global warming, and the synchronicity of the increased El Niño periods with the accelerated recession of the Mt. Jaya glaciers over the past quarter of a century suggests that the glaciers will continue to recede at high rates over the near future. Using a conservative rate of recession calculated from ice losses over the period of 1972-2005, the Carstensz glacier system, the E. Northwall/Meren system, and the W. Northwall Firn will be gone in approximately 21, 14 years, and 2.5 years, respectively. If El Niño frequency and magnitude continues to increase, a rate of recession calculated from 1987-2005 could still be considered conservative. Using this rate only slightly changes the prediction for the E. Northwall/Meren system and the W. Northwall Firn. However,

utilizing the 1987-2005 rate of recession the Carstensz glacier system will be gone in approximately 11.5 years.

REFERENCES

Allison, I. 1974. Morphology and dynamics of the tropical glaciers of Irian Jaya. *Z. Gletscherkd. Glazialgeol*., **10**(1-2), 129-152.

Allison, I. and J. Bennett. 1976. Climate and microclimate. *In* Hope G.S., J.A. Peterson, U. Radok, and I. Allison, *eds*. *The equatorial glaciers of New Guinea – results of the 1971-1973 Australian Universities' expeditions to Irian Jaya: survey, glaciology, meteorology, biology, and paleoenvironments.* Rotterdam, A.A. Balkema, 61-80.

Allison, I. and P. Kruss. 1977. Estimation of recent climate change in Irian Jaya by numerical modeling of its tropical glaciers. *Arct. Alp. Res*., **9**(1), 49-60.

Allison, I. and J.A. Peterson. 1976. Ice areas on Puncak Jaya – their extent and recent history. *In* Hope G.S., J.A. Peterson, U. Radok, and I. Allison, *eds*. *The equatorial glaciers of New Guinea – results of the 1971-1973 Australian Universities' expeditions to Irian Jaya: survey, glaciology, meteorology, biology, and paleoenvironments.* Rotterdam, A.A. Balkema, 27-38.

Allison, I. and J.A. Peterson. 1989. Glaciers of Irian Jaya, Indonesia. *In* Williams, R.S., Jr and J.G. Ferrigno, *eds*. *Satellite image atlas of glaciers of the world.* Washington DC, US Government Printing Office. (US Geological Survey Professional Paper 1386-H.)

Braithwaite, R.J. and Y. Zhang. 1999. Modeling changes in glacier mass balance that may occur as a result of climate changes. *Geogr. Ann.*, **81**, 489-496.

Dozy, J.J. 1938. Eine Gletscherwelt in Niederländisch-Neuguinea. *Zeitschrift für Gletscherkunde, für Eiszeitforschung und Geschichte des Klimas,* **26**(1-2), 45-57.

Dyurgerov, M.B. and M.F. Meier. 2000. Twentieth century climate change: evidence from small glaciers. *Proceedings of the National Academy of Sciences of the United States of America,* **97**(4), 1406-1411.

Earth Remote Sensing Data Analysis Center (ERSDAC). Accessed December 2006. *ASTER reference guide*. Version 1.0. http://www.science.aster.ersdac.or.jp/en/documnts/pdf/ASTER_Ref_V1.pdf.

Favier, V., P. Wagnon, J.P. Chazarin, L. Maisincho and A. Coudrain. 2004a. One-year measurements of surface heat budget on the ablation zone of Antizana Glacier 15, Ecuadorian Andes. *J. Geophys. Res*., **109**, D8105. (10.1029/2003JD004359.)

Favier, V., P. Wagnon and P. Ribstein. 2004b. Glaciers of the outer and inner tropics: a different behavior but a common response to climatic forcing. *Geophys. Res. Lett*., **31**(16), L16403. (10.1029/2004GL020654.)

Francou, B., P. Ribstein, R. Saravia and E. Tiriau. 1995. Monthly balance and water discharge of an inter-tropical glacier: Zongo glacier, Cordillera Real, Bolivia, 16°S. *J. Glaciol.*, **41**(137), 61-67.

Francou, B., M. Wuille, P. Wagnon, J. Mendoza and J.E. Sicart. 2003. Tropical climate change recorded by a glacier in the central Andes during the last decades of the twentieth century: Chacaltaya, Bolivia, 16°S. *J. Geophys. Res*. **108**(D5), 4154. (10.1029/2002JD002959.)

Francou, B., M. Vuille, V. Favier and B. Cáceres. 2004. New evidence for an ENSO impact on low-latitude glaciers: Antizana 15, Andes of Ecuador, 0°28'S. *J. Geophys. Res*., **109**(D18), D18106. (10.1029/2003JD004484.)

Garreaud, R., M. Vuille, and A.C. Clement. 2003. The climate of the Altiplano: observed current conditions and mechanisms of past changes. *Palaeogeogr., Palaeoclimatol., Palaeoecol.*, **194**: 5-22.

GeoEye. Accessed on December 17, 2006. IKONOS product guide. http://www.geoeye.com/techpapers/default.htm.

Georges, C. 2004. 20th-Century glacier fluctuations in the tropical Cordillera Blanca, Peru. *Arct., Antarct., Alp. Res*., **36**(1): 100-107.

Grodecki, J. and G. Dial. 2001. IKONOS geometric accuracy. *Proceedings of Joint Workshop of ISPRS Working Groups I/2, I/5, and IV/7 on High Resolution Mapping From Space 2001*. University of Hanover, Hanover, Germany. Sept. 19-21, 2001.

Harrer, H. 1965. *I come from the Stone Age*. New York, E.P. Dutton.

Hastenrath, S. and P.D. Kruss. 1992. Greenhouse indicators in Kenya. *Nature*, **355**(6360), 503-504.

Haverkamp, D. and R. Poulsen. 2003. Change detection using IKONOS imagery. *ASPRS 2003 Annual Conference Proceedings*. Anchorage, Alaska.

Hope G.S., J.A. Peterson, U. Radok, and I. Allison. 1976. *The equatorial glaciers of New Guinea – results of the 1971-1973 Australian Universities' expeditions to Irian Jaya: survey, glaciology, meteorology, biology, and paleoenvironments*. Rotterdam, A.A. Balkema.

Houghton, J.T., Y. Ding, D.J. Griggs, M. Noguer, P.J. van der Linden and 3 others, eds. 2001. *Climate change 2001: the scientific basis.* Contribution of Working Group I to the Third Assessment Report of the Intergovernmental Panel on Climate Change. Cambridge, etc., Cambridge University Press.

Jensen, J.J. 2000. *Introductory digital image processing: a remote sensing perspective.* 3rd Edition. Upper Saddle River, New Jersey, Pearson Prentice Hall.

Kaser, G. 1999. A review of the modern fluctuations of tropical glaciers. *Global Planet. Change*, **22**(1-4), 93-103.

Kaser, G. 2001. Glacier-climate interaction at low latitudes. *J. Glaciol*., **47**(157), 195-204.

Kaser, G. and H. Osmaston. 2002. *Tropical glaciers*. Cambridge, Cambridge University Press.

Klein, A.G. and J.L. Kincaid. 2006. Retreat of glaciers on Puncak Jaya, Irian Jaya, determined from 2000 and 2002 IKONOS satellite images. *J. Glaciol*., **52**(176), 65-79.

Klein, A.G., G.O. Seltzer, and B.L. Isacks. 1999. Modern and last local glacial maximum snowlines in the Central Andes of Peru, Bolivia, and Northern Chile. *Quat. Sci. Rev*., **18**, 63-84.

Mercer, J.H. 1967. *Southern hemisphere glacier atlas.* Natick, Massachusetts, US Army Natick Laboratories. (Technical Report. 67-76-ES.)

Mölg, T. and D.R. Hardy. 2004. Ablation and associated energy balance of a horizontal glacier on Kilimanjaro. *J. Geophys. Res. Atmos*. **109**, (D16104). (10.1029/2003JD004338.)

Mölg, T., D.R. Hardy and G. Kaser. 2003. Solar-radiation-maintained glacier recession on Kilimanjaro drawn from combined ice-radiation geometry modeling. *J. Geophys. Res.*, **108**(D23), 4731. (10.1029/2003JD003546.)

National Aeronautics and Space Administration (NASA). Accessed December 2006a. *ASTER: Advanced Spaceborne Thermal Emission and Reflection Radiometer.* http://asterweb.jpl.nasa.gov/.

National Aeronautics and Space Administration (NASA). Accessed December 2006b. Earth Observing System Data Gateway. http://edcimswww.cr.usgs.gov/pub/imswelcome/.

National Aeronautics and Space Administration (NASA). Accessed December 2006c. *Landsat 7: science data users' handbook.* http://landsat.gsfc.nasa.gov/data/sci_data.html.

National Oceanic and Atmospheric Administration - Cooperative Institute for Research in Environmental Sciences (NOAA-CIRES). Accessed April 2005. NCEP Reanalysis data provided by the NOAA-CIRES Climate Diagnostics Center, Boulder, Colorado, USA. http://www.cdc.noaa.gov/.

Peterson, J.A., G.S. Hope and R. Mitton. 1973. Recession of snow and ice fields of Irian Jaya, Republic of Indonesia. *Z. Gletscherdk Glazialgeol*., **9**(1-2), 73-87.

Peterson, J.A. and L.F. Peterson. 1994. Ice retreat from the neoglacial maxima in the Puncak Jayakesuma area, Republic of Indonesia. *Z. Gletscherdk Glazialgeol*., **30**, 1-9.

Prentice, M.L., G.S. Hope, K. Maryunani, and J.A. Peterson. 2005. An evaluation of snowline data across New Guinea during the last major glaciation, and area-based glacier snowlines in the Mt. Jaya region of Papua, Indonesia, during the Last Glacial maximum. *Quat. Int.* **138-139**, 93-117.

Ramírez, E., B. Francou, P. Ribstein, M. Descloitres, R. Guérin and 4 others. 2001. Small glaciers disappearing in the tropical Andes: a case study in Bolivia: Glacier Chacaltaya (16°S). *J. Glaciol*. **47**(157), 187-194.

United States Geological Survey (USGS). Accessed on December 2006. Earth Resources Observation and Science. http://edcsns17.cr.usgs.gov/EarthExplorer/.

Wagnon, P., J.E. Sicart, E. Berthier and J.P. Chazarin. 2003. Wintertime high-altitude surface energy balance of a Bolivian glacier, Illimani, 6340m above sea level. *J. Geophys. Res.*, **108**(D6), 4177. (10.1029/2002JD002088.)

Wollaston, A.F.R. 1914. An expedition to Dutch New Guinea. *Geogr. J.*, **43**(3), 248-268.

VITA

Name: Joni L. Kincaid

Address: Texas A&M University, Department of Geography
810 O&M Building, TAMU Mail Stop 3147,
College Station, Texas 77843-3147

Education: B.A., Geography (2003), The University of Texas, Austin, Texas
M.S., Geography (2007), Texas A&M University, College Station, Texas

Publications:

Kincaid, J.L. and A.G. Klein. 2004. Retreat of the Irian Jaya glaciers from 2000 to 2002 as measured from IKONOS satellite images. Proceedings of the 61st Annual Eastern Snow Conference.

Klein, A.G. and J.L. Kincaid. 2006. Retreat of glaciers on Puncak Jaya, Irian Jaya, determined from 2000 and 2002 IKONOS satellite images. *J. Glaciol*., **52**(176), 65-79.

Klein, A.G., and J.L. Kincaid, and K.E. Merritt. 2006. Assessing the accuracy of mapping small tropical glaciers: a comparison of glacier mapping techniques applied to the glaciers on Mt. Jaya, Irian Jaya. Submitted to *Remote Sens. Environ*.

Professional Presentations:

The 61st Annual Eastern Snow Conference. Portland, Maine. 2004.

European Association of Remote Sensing Laboratories. Bern, Switzerland. 2005.

The Southwestern Division of the Association of American Geographers. Fayetteville, Arkansas. 2005.

American Geophysical Union Fall Meeting. San Francisco, California. 2005.

Annual Meeting for GK-12 Project Teams. Washington D.C. 2006.

Global Land Ice Measurement from Space Workshop. Cambridge, United Kingdom. 2006.

Professional Experience:

Graduate Teaching Assistant – GEOG 203 (Fall 2003- Spring 2004)
Department of Geography, Texas A&M University, College Station, Texas.

Graduate Research Assistant – Dr. Eric Lindquist (Spring 2004-Summer 2005)
The Institute for Science, Technology, and Public Policy, The Bush School, Texas A&M University, College Station, Texas.

Graduate Research Assistant – Dr. Andrew Klein (Summer 2004-Summer 2005)
Department of Geography, Texas A&M University, College Station, Texas.

National Science Foundation Fellow – Advancing Geospatial Skills in Science and Social Science (Fall 2005-Spring 2007). Department of Geography, Texas A&M University, College Station, Texas.